

Not peer reviewed
Submitted to Journal of Hydrology for peer review

Information Content of Hydrologic Data across Space: Streamflow Predictions using Machine Learning

Abhinav Gupta*

Division of Hydrologic Sciences, Desert Research Institute, Las Vegas, NV, USA

*abhinav.gupta@dri.edu

Highlights

1. A large library of watershed hydrologic data is useful to model streamflow dynamics
2. But for a specific watershed, information from a few nearby watersheds is sufficient
3. The prevalent idea is that an LSTM should be trained with data across hundreds of watersheds
4. Based on the results of this study, the above idea appears to be baseless
5. LSTM trained using data across several watersheds may become excessively sensitive to rainfall

****This paper has not been peer reviewed and has been submitted to the Journal of Hydrology for peer review. The present version is a preprint submission to EarthArXiv.**

Abstract

This study aimed to assess the usefulness of data from donor watersheds to predict streamflow in parent watersheds. For this purpose, Long-Short Memory Network (LSTM) is used as an information extraction algorithm. Data from a total of 434 watersheds were used in this study. Out of these 434 watersheds, 57 watersheds were selected as the parent watersheds. These 57 watersheds were those where streamflow statistical structure changed over the study period (1980-2013 water years). Several LSTM models were developed by using the different number of donor watersheds as training watersheds varying from 1 to 128. It was found that the optimal number of training watershed were much less than 128 for most of the parent watersheds. Increasing the number of donor watersheds beyond this optimal value resulted in a statistically insignificant gain in accuracy. In some cases, the Nash-Sutcliffe Efficiency (NSE) decreased, albeit only slightly, when the number of donor watersheds for training increased beyond the optimal value. However, we also found that using data from more watersheds beyond the optimal number of training watersheds results only in a slight decrease in NSE. Therefore, one bears only a small cost by training LSTM against a large number of watersheds compared to the optimal number of watersheds. The results of this study contradict the prevalent idea that LSTM continues to extract hydrologically relevant information as more and more data are fed to the model; this was true only for a few of the 57 parent watersheds used in this study.

Keywords: Hydrologic Information; Streamflow; Rainfall-Runoff Modeling; Long-Short Memory Network (LSTM); Machine Learning

1. Introduction

1.1 Machine learning and data across several different watersheds

Recently, machine learning (ML) has gained popularity among hydrologists (Karpatne, 2018; Kratzert et al., 2018a; Kratzert et al., 2018b; Chandawala et al., 2019; Kratzert et al., 2019a; Kratzert et al., 2019b; Bennet & Nijssen, 2020; Dutta and Maity, 2020; Konpala et al., 2020; Fang et al., 2021; Gauch et al., 2021a; Gauch et al., 2021b; Herath et al., 2021; Lee et al., 2021; Razavi 2021; Sadler et al., 2022). In some studies, ML has been used as a tool for searching some optimal conceptual/process-based representation of a watershed hydrologic system (e.g., Chandawala et al., 2019), but in most of the recent studies, Long-Short Memory Network (LSTM; a variant of recurrent neural networks which is especially suitable for time series prediction) has been used to predict streamflow.

The use of ML algorithms is not new in hydrology. Several earlier studies have reported the ability of ML models including neural networks (e.g., Govindaraju, 2000; Zhang and Govindaraju, 2000; Zhang and Govindaraju, 2003) and regression trees (e.g., Iorgulescu and Beven, 2004) to predict streamflow. These studies trained ML models using data only from the watershed where the streamflow predictions were to be made. On the other hand, ML's recent popularity in hydrology is due to its ability to use data across several watersheds to learn the rainfall-runoff relationships

(Kratzert et al., 2019b & 2019c). Based on the comparison of NSE values (and some other goodness-of-fit measures) obtained by these models, it has been shown that LSTMs can give better predictions of streamflow than those obtained by conceptual and process-based hydrologic models (e.g., Lees et al., 2021; Kratzert et al., 2019c). But the question remains how much *information* an ML algorithm such as LSTM can extract from hydrologic data across different watersheds? The word ‘information’ here is used in the context of streamflow prediction. More specifically, how much improvement in streamflow prediction accuracy is obtained when data across several watersheds are used to train an LSTM compared to when data from only one or a few watersheds are used?

Some authors have recently addressed this question. Fang et al., (2022) argued that using data across several *diverse* watersheds to train an ML model tends to yield better streamflow predictions than those obtained by an ML model trained using the data across *similar* watersheds. Also, Gauch et al., (2021) argued that using data from a large number of *randomly selected* watersheds yields better streamflow predictions than those obtained using data from a few watersheds. They claim that better streamflow predictions are obtained as more data are used to train an ML model. Specifically, these authors concluded that streamflow prediction improves by training the LSTM on more data even after data from hundreds of watersheds have already been used to train the model.

Nash-Sutcliffe Efficiency (NSE), which is known to be very sensitive to prediction improvements even at a few time steps (Clark et al., 2021), is typically used for model comparisons. However, it is not quite clear how much improvement in the predictions can be obtained by using data from more and more watersheds and if the improvement obtained is statistically significant. Researchers have also attempted to assess the improvement in streamflow prediction accuracy when LSTM is trained against more and more temporal observations in a given watershed. A notable example is a recent study by Boulmaiz et al. (2020) where an LSTM model was trained with different lengths of data (3, 6, 9, 12, and 15 years) to predict streamflow, and the NSE kept increasing as training data length increased. Figure 8 of their study shows that in one of the studied catchments NSE improved from 0.71 to 0.83 as training data length increased from 6 to 15 years. But the improvement mainly occurred in terms of better prediction of two streamflow peaks. Thus, should the improvement in NSE from 0.71 to 0.83 be considered significant or marginal? As noted by these authors, such improvements should be met with skepticism given the uncertainty in rainfall (Renard et al., 2011; Bardossy and Anwar, 2022, preprint) and streamflow data (Le Coz et al., 2014). Note that the studies mentioned above do not systematically account for uncertainty in NSE.

1.2 Predictions under non-stationarity

The potential of ML models to extract hydrologically relevant information from different watersheds may prove to be effective for streamflow prediction under climate-induced non-stationarities (Milly et al., 2008). Most process-based and conceptual hydrologic models need to

be calibrated against historical hydrologic observations. The parameters thus calibrated depend upon the data used and may result in poor predictions in the presence of climate change (Stephens et al., 2020). ML can address this problem if the rainfall-runoff dynamics of a watershed after climate change become similar to the rainfall-runoff dynamics of some other watersheds in the training set before climate change. This idea is formally referred to as space-time symmetry (Sivapalan et al., 2011; Singh et al., 2012) – equivalence of temporal and spatial variability.

Nearing et al., (2019) showed that an ML model can be trained to be sensitive to background climate (represented by the annual mean precipitation, the temperature of the last 365 days, etc.). They cite the ability of ML to ‘see everything’ (which is essentially space-time symmetry) as the reason for this. Wi and Steinschneider (2022) showed that ML models can yield physically realistic responses to an increase in mean temperatures where physical realism was assessed by a model’s ability to simulate decreased runoff-ratios (except in glacier-dominated regions) and an increase in winter runoff in response to increased temperatures. These authors also argued that an ML model is physically more realistic when it is trained using data across several watersheds (531 in their study). Further, these authors found that different models including process-based models and ML models with different training data had very different responses to an increase in temperature even though all these models had similar performance in terms of streamflow prediction.

It is, however, not shown if the response of ML models to climate change is aligned with the *observed* response of watersheds to climate change. This is difficult to show because one must know beforehand which watershed has experienced *hydrologic regime* change due to climate change. Hydrologic regime here refers to either the change in streamflow statistical structure or change in rainfall-runoff response of a watershed or both. It is essential to test the ability of ML models to yield good predictions of streamflow in watersheds where we expect that a change in the hydrologic regime has occurred.

1.3 Study objectives

The objective of this study is to test how much information can an ML algorithm extract from data across different watersheds to predict streamflow. Specifically, we want to find out the *optimal* number of watersheds required to train an LSTM model to predict streamflow in a given watershed. The meaning of the term ‘optimal’ would become clear in what follows.

We also wanted to assess the usefulness of the data across different watersheds in predicting streamflow under the climate-induced non-stationarities. Therefore, watersheds to test the first objective were selected such that these watersheds experienced a change in streamflow statistical structure (SSS; Gupta et al., 2022, preprint) over the period of this study (1980-2013 water years) were studied. Further, the changes in SSS of these watersheds were related to the changes in precipitation and temperature statistics (Gupta et al., 2022, preprint). The rationale behind using the change in SSS to select the test watersheds is provided below.

2. Study area

Catchment Attributes and Meteorology for Large Sample studies (CAMELS; Addor et al., 2017a; Addor et al., 2017b; Newman et al., 2014; Newman et al., 2015) dataset was used in this study. This dataset contains data on 27 catchment attributes (soil properties, vegetation characteristics, topography, static climate characteristics such as aridity index) and 5 meteorological variables at the daily scale (precipitation, minimum temperature, maximum temperature, vapor pressure, relative humidity) along with daily streamflow data. This dataset has been used in several other large sample studies in recent years. The watersheds contained in the dataset have minimal direct anthropogenic disturbances.

This dataset contains data from a total of 671 watersheds across the USA. Out of these 671, 531 watersheds were initially selected for this study based on Kratzert et al., (2019c). Further filtering was done based on the changes in the *statistical structure of streamflow* time-series (Gupta et al., 2022, preprint). Here, we define streamflow statistical structure as the contribution of different components of streamflow to the streamflow total variance. The different components include ‘less than 2-weeks timescale’, ‘2-weeks to 1-month timescale’, ‘1-month to 4-months timescale’, ‘4-months to 1-year timescale’, and ‘greater than 1-year timescale’. Only the watersheds where the contribution of less than 2-weeks timescale component changed significantly over the study period and the ones where no change occurred were selected for this study (details are provided in Gupta et al., 2022, preprint). A total of 434 such watersheds were found in this study. The watersheds with changes in the contributions of the other components were filtered out since there is strong correlation between the changes in various components. Further, rationale for this filtering procedure is provided below.

3. LSTM configuration, numerical experiments, and model comparison

Data from all the watersheds were divided into three sub-periods: training, validation, and testing (Hastie et al., 2009). The methodology of Kratzert et al., (2019c) was followed to train the LSTM models. To predict streamflows at a time step, the previous 365 days of meteorological data were fed to the LSTM model along with static watershed attributes. One LSTM layer with the hidden layer size of 256 was used. Outputs from the LSTM layer were fed to a fully connected layer which yields the final output. During the training phase, 40% of the neurons in the fully connected layer were dropped randomly to prevent overfitting (Srivastava et al., 2014). Each model was trained for 50 epochs with a minibatch size of 256. Weights corresponding to the epoch with maximum NSE on the validation set were kept as final trained weights. For a given training data, 8 different models were trained with different random seeds to alleviate the effect of randomness in model training. The loss function used was $1 - NSE$ (where NSE was computed as in Kratzert et al., 2019c). The average of the streamflows obtained by the 8 models was treated as the final streamflow prediction. For comparisons with other studies, this model configuration was tested in terms of reproducing the results reported by Kratzert et al., (2019c). This configuration yielded NSE values almost identical to those reported by Kratzert et al., (2019c) affirming that this configuration is suitable for this study.

We compared the NSEs obtained by the configuration discussed above with another configuration where the size of the LSTM hidden layer was 312. Increasing the hidden layer size did not yield any improvement in accuracy, therefore, the hidden layer size was chosen to be 256. More discussion on hyperparameter tuning is provided below in Section 6.

Six experiments were carried out. In each experiment, several LSTM models were trained using different sizes of training data by varying the number of watersheds used for training. The number of watersheds used for training was 1, 2, 4, 8, 16, 32, 64, 90, 128, and 434. From each watershed, the daily data from water years 1980-1989 were used for training. All the models were validated using the daily data from water years 1991 to 1995 and tested using daily data from 2001 to 2013 water years (the rationale for selecting these time periods is given below). Nine years of training data from each watershed is justified because LSTMs are typically able to extract all the hydrologically relevant information about rainfall-runoff dynamics from 9 years of training data (Gauch et al., 2021) – increasing the length of the training period further does not usually result in better performance.

The six experiments varied in terms of how the training watersheds were selected. In general, $n = 1, 2, 4, \dots, 434$ watersheds were selected based on their *similarity* with test watersheds, i.e., n watersheds most similar to the test watersheds were selected. The similarity was computed between the test period (2001-2013 water years) of test watersheds and the training period (1980-1989 water years) of training watersheds. The first three experiments were designed to test the usefulness of data across several watersheds in training an ML model when the prediction is to be made at a gauged location. The other three experiments were designed to test the usefulness of data across several watersheds in training an ML model when the prediction is to be made at an ungauged location.

Since training an LSTM model takes large computational time depending upon the amount of data (number of watersheds) used for training, it is prohibitive to train 80 (10 sets of training watersheds \times 8 different random seeds for each set of training watersheds) different models for each of the watersheds as test watershed used in this study. Therefore, 57 watersheds were selected as the test watersheds for this study based on the changes in streamflow statistical structure (Figure 1). Basically, out of the 434 watersheds used in this study, these 57 test watersheds had statistically significant changes in the contribution of high frequency (less than 2-week timescales) components to total streamflow variance. These authors also hypothesized that the change in streamflow statistical structure was related to the change in climatic statistics. Thus, it is reasonable to assume that in these 57 test watersheds hydrologic regime has changed over the study period due to climate change. Further, it was observed that the change in streamflow statistical structure was gradual and consistent in most of these watersheds. Thus, the earliest nine and the latest thirteen water years can be assumed to have different hydrologic regimes.

It is still computationally prohibitive to develop 80 LSTM models for each of the 57 test watersheds, separately. Therefore, these 57 test watersheds were grouped into 10 clusters using k-

means clustering based on their static attributes (Figure 1). For each cluster, one model was trained using data from n watersheds. Thus, a total of 721 (10 clusters \times 9 sets of watersheds for training \times 8 random seeds + 1 model using training period data from all 434 watersheds) LSTM models were trained in each experiment.

The scheme mentioned above for selecting test watersheds was used to address the second objective, albeit with some limitations as discussed below. Systematic changes in rainfall and temperature patterns have been observed in several CAMELS watersheds over the study period (water years 1980-2013). But the change in these climatic statistics in a watershed does not necessarily result in a change in the hydrologic regime of the watershed or a change in the streamflow statistical structure. Therefore, change in streamflow statistical structure was used as a measure to select the 57 test watersheds that are used in this study. A detailed analysis describing the change in streamflow structure in the CAMELS watersheds is presented in Gupta et al., (2022, preprint).

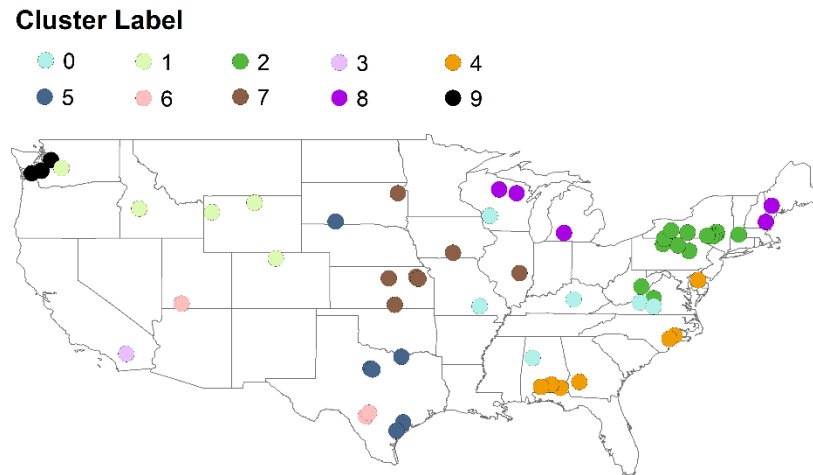


Figure 1. Location of the 57 test watersheds. The color scheme illustrates the clustering of the 57 watersheds based on static attributes: watersheds belonging to the same cluster are represented by the same color. Note that watersheds belonging to the same cluster are close to each other in space with a few exceptions.

The details of the six experiments are as follows:

Experiment 1: Training watersheds were selected based on the similarity of their climate with *cluster climate*. Training period data from watersheds contained in the cluster were also used to train the model. For example, if a cluster has k number of watersheds, then 10 models were trained with $k + n$ watersheds, where $n = 1, 2, 4, 8, 16, 32, 64, 90, 128, (434 - k)$. The n donor watersheds were selected from the remaining $(434 - k)$ watersheds.

Climate similarity was computed in the space of the following climatic statistics: the average number of storms per day, the mean storm depth, the fraction of precipitation days, the fraction of high precipitation days, the fraction of low precipitation days, the average high precipitation duration, the average low precipitation duration, the mean high precipitation depth, the mean low

precipitation depth, the mean high precipitation frequency, the mean low precipitation frequency, the mean seasonal precipitation depth, the mean seasonal minimum, and maximum temperatures. These climatic statistics were computed separately for the training and testing periods, i.e., two sets of climatic statistics were computed for a given watershed: one set for the training period and the other set for the testing period. The climatic statistics in the training and testing periods could be different because of climate change. Cluster climate was defined by the mean of the climatic statistics of the watersheds contained in a cluster. For a given cluster containing k watersheds where streamflow is to be predicted during the years 2001 to 2013, n donor watersheds (out of the remaining $(434 - k)$ watersheds) that had training period climatic statistics closest to the testing period climatic statistics of the cluster were chosen. The similarity was computed as the Mahalanobis distance between two points in climatic statistics space: the smaller the Mahalanobis distance higher the similarity.

Experiment 2: Training watersheds were selected based on the similarity of their static attributes with cluster static attributes. Training period data from watersheds contained in the cluster were also used to train the model. Static attributes used in this study include soil properties, geological permeability, vegetation properties such as the fraction of forest, and the long-term climate such as aridity. A detailed list of static attributes is provided in Appendix A. Again, the similarity was computed based on the Mahalanobis distance between two points in the static attribute space.

Experiment 3: Training watersheds were selected based on the similarity of their climatic statistics and static attributes with test watershed climatic statics and static attributes. The training period data from the test cluster were also used to train the models. The climatic statistics and static attributes used in this experiment were the same as those used in experiment 1 and experiment 2, respectively. The similarity was computed using the expression

$$d_{cs} = (d_c^2 + r^2 d_s^2)^{\frac{1}{2}}, \quad (1)$$

where d_{cs} denotes the distance between two points in combined climatic and static attribute space, d_c denotes the distance between the two points in climatic space, d_s denotes the distance between the two points in static attribute space, and r is the ratio of the number of the climatic statistics to the number of the static attributes. The ratio r is used so that the contribution of climatic and static attributes is equal in computing the similarity. One may use any other value of $r \in [0,1]$ to vary the importance given to climatic and static attributes in computing similarity.

Experiment 4: Same as experiment 1 except that the training period data from test cluster watersheds were not used.

Experiment 5: Same as experiment 2 except that the training period data from test cluster watersheds were not used.

Experiment 6: Same as experiment 3 except that the training period data from test cluster watersheds were not used.

Note that difference within the experiments 1-3 lies in the way the donor watersheds are selected for training. In experiments 1, 2, and 3, the climatic similarity, the watershed static attribute similarity, and a combination of climatic statistics and static attribute similarity were used, respectively. Perhaps, a more appropriate way of computing the distance metrics is to assign different weights to different attributes, for example, using principal component analysis (PCA). Therefore, we repeated experiment 1 for cluster 1 by computing distance metric in PCA space. But minimal changes were found in the results; therefore, all the attributes were weighted equally in this study.

The performance of the two models in terms of streamflow prediction was assessed on the test data using the popularly used Nash Sutcliff Efficiency (NSE) metric. NSE can be very sensitive to improvement in predictions at a few time steps (Clark et al., 2021). Thus, out of the two models that give similar predictions at most of the time steps, the one model that gives better predictions at a few time steps may be wrongly identified as a significantly better model. To tackle this problem, the probability distributions over NSE values were computed using a bootstrap method. This allows us to determine if the difference between the two given models is statistically significant. For each model, a total of 1000 bootstrap samples were drawn using 1000 prefixed random seeds.

Statistical significance of the two LSTM models trained using k_1 (model 1) and k_2 (model 2) watersheds with $k_2 > k_1$ was computed as follows. Let $p_{\text{diff}}(\text{NSE})$ denote the probability density of difference in NSEs obtained by model 2 and model 1. Model 1 can be considered statistically indistinguishable from model 2, in terms of NSEs, at α significance level if the p_s value computed using

$$p_s = P_{\text{diff}}(\text{NSE} < 0) \quad (2)$$

is greater than α . Here, P_{diff} is the probability mass associated with the density p_{diff} . Similarly, the difference between NSEs obtained by model 2 and model 1 can be considered statistically significant at the α significance level if the p_s computed using (2) is smaller than the α . In this study, the value of $\alpha = 0.05$ was chosen. Note that it is assumed in Equation (2) that the mean NSE obtained by model 2 is greater than the mean NSE obtained by model 1. Using this procedure, the minimum number of basins required to train an LSTM model which yielded an NSE value statistically indistinguishable from the NSE value yielded by the ‘best’ LSTM model was determined. Here, the best LSTM model is the one with the highest NSE value. This minimum number of watersheds is referred to as the optimal number of watersheds in this study. For all the experiments, NSEs computed over the test period were compared.

In what follows, the following terms and notations are used for ease of exposition:

Parent watersheds: Includes watershed A where streamflow is to be predicted and the watersheds contained in the cluster to which watershed A belongs.

Donor watersheds: Watersheds except for parent watersheds which are or can be used to train the model.

N_T : Number of donor watersheds used to train an LSTM model.

Also, different hydroclimatic regions of the USA will be referred to. These regions are shown in Figure A1. Further, the terms ‘parent watersheds’ and ‘test watersheds’ have been used interchangeably.

4. Results

4.1 Experiments at gauged locations

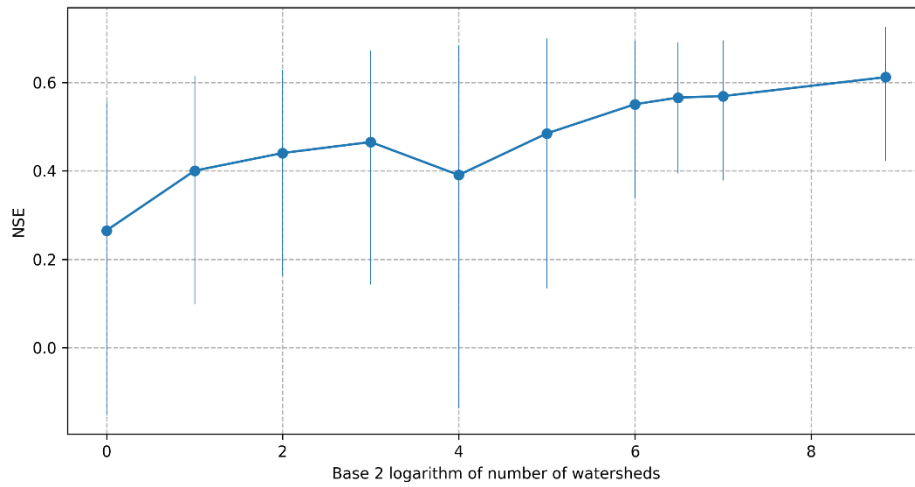
First, we illustrate the procedure to compute optimal N_T . Figure 2 shows the change in test NSE values, along with the 95% confidence intervals, as more and more watersheds are used for training the LSTM model for six watersheds belonging to different clusters. These results are for the experiment 1 where the similarity between watersheds was decided based on climatic statistics. The six watersheds in Figure 2 illustrate all the different qualitative behaviors of NSE vs. N_T plots. The mean NSE increases in all the watersheds as N_T increases from 0 to 64. For the higher value of N_T , the change in NSE is different in different watersheds. In Figures 2a and 1e, NSE seems to have reached a plateau at $N_T = 64$. In Figure 2b, NSE starts to decrease after $N_T = 64$. In Figure 2c, NSE increases up to $N_T = 128$ and decreases afterward. In Figures 2d and 1f, NSE keeps increasing up to $N_T = 434$.

The uncertainty in NSE values is very high. It is clear in Figure 2a that NSE obtained using $N_T = 64$ are statistically indistinguishable from the NSEs obtained by using all the 434 watersheds for training. Analysis revealed that the NSEs obtained using $N_T = 8$ were statistically indistinguishable from the NSEs obtained using $N_T = 434$ at the 5% significance level in Figure 2a. This implies that using more than 8 training watersheds results in streamflow prediction improvement but only at a few time steps. Thus, the optimal N_T value in this particular watershed is 8. It is noteworthy that the mean NSEs obtained using $N_T = 8$ and $N_T = 434$ are quite different (NSE = 0.46 with $N_T = 8$ and NSE = 0.60 with $N_T = 434$) in this watershed. Also, it is clear that at the 10% significance level optimal N_T would be either 32 or 64. In summary, the optimal value of N_T is much smaller than 434.

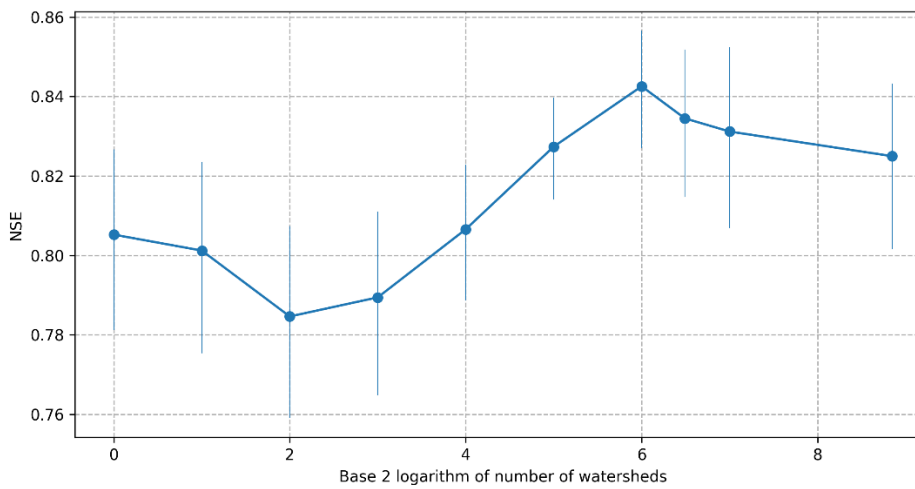
In Figures 2b, 2c, and 2d, the optimal N_T values are 64, 128, and 128, respectively. These values of N_T also yield the highest mean NSE. In Figures 2f, the optimal $N_T = 434$, and it seems that if more watersheds were used for training NSE would have further improved in this watershed. In Figure 2e, the mean NSE increases as N_T increases from 1 to 434 but the uncertainty in NSE is so high that optimal N_T is equal to 1.

Out of all the 57 test watersheds, there were only two watersheds where optimal N_T was equal to 434. These are shown in Figures 2d and 1f. In Figure 2d, the difference between NSEs obtained by using N_T equal to 434 and 128 was negligible (equal to 0.025). In summary, except for these

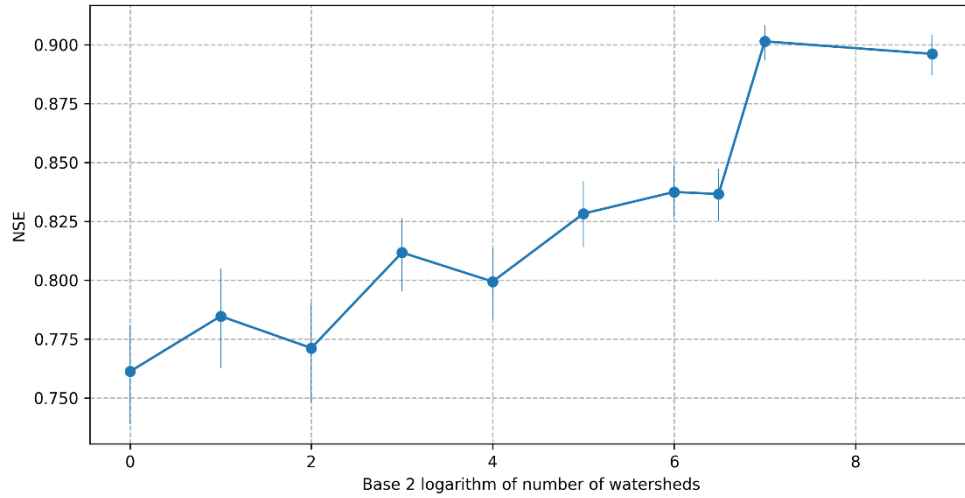
two watersheds, there was no improvement in NSE if N_T was increased beyond 128. Therefore, in what follows, the analysis was carried out for n varying from 1 to 128. This decision was made to save time in LSTM model training in experiments 4, 5, and 6.



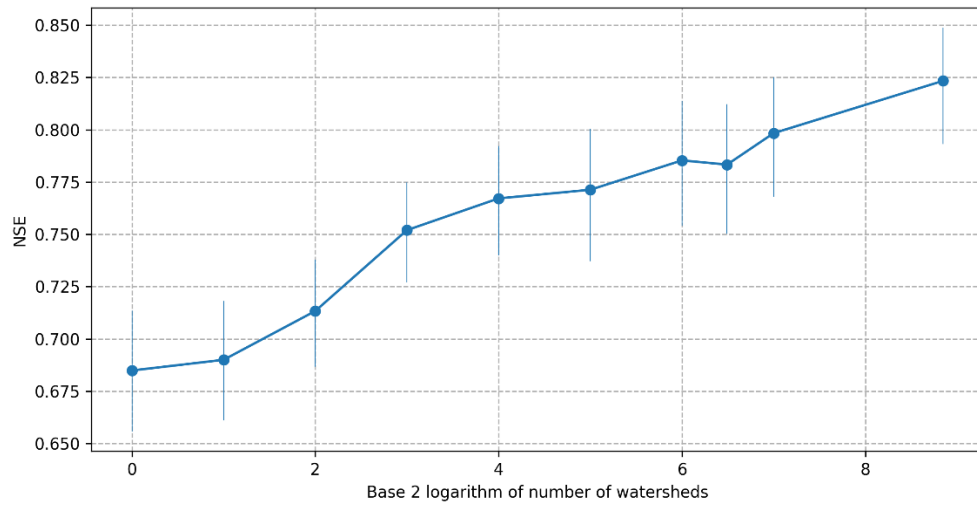
(a)



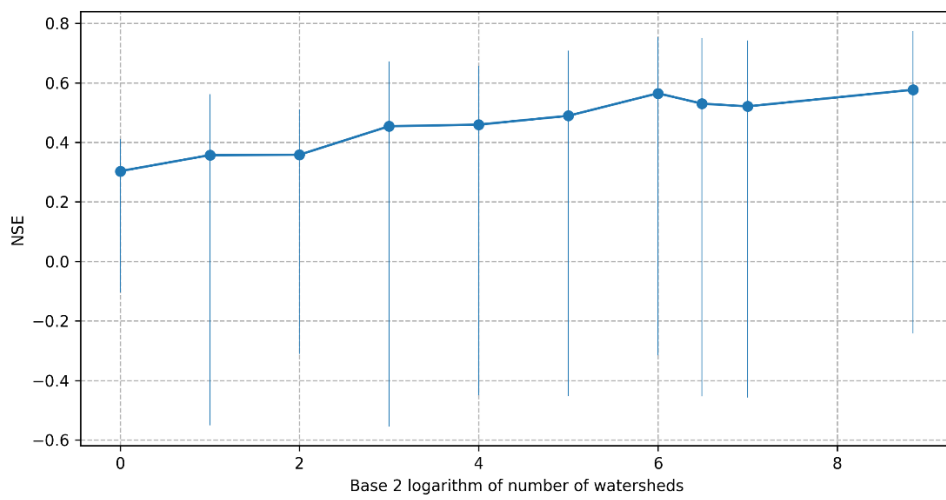
(b)



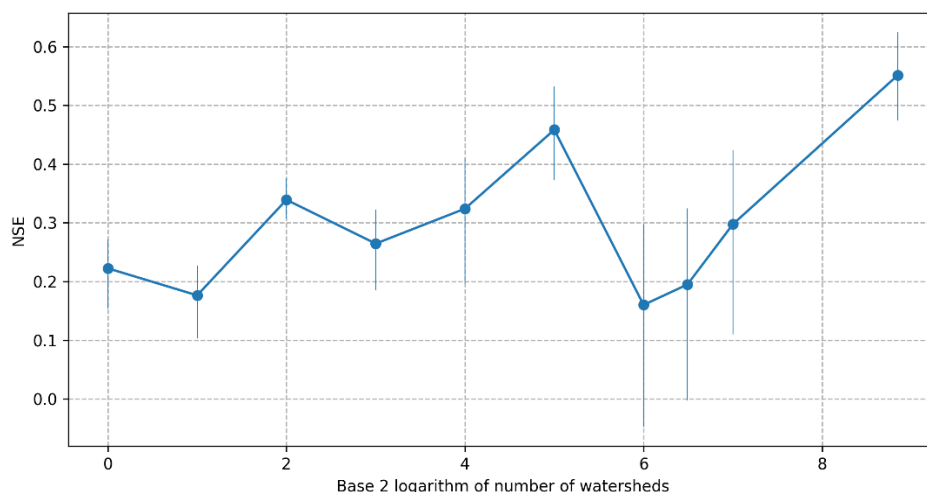
(c)



(d)



(e)



(f)

Figure 2. *Experiment 1.* Change in model performance in terms of Nash-Sutcliffe Efficiency (NSE) as data from more and more donor watersheds are used to train the LSTMs. The vertical bars represent the 2.5th (lower limit) to the 97.5th (upper limit) percentile of the NSE values. These NSEs are for the test period 2001-2013 water years.

Figure 3 shows the optimal N_T values corresponding to each of the 57 test watersheds. The optimal N_T value is less than 8 for many watersheds located in Texas, Southern California, and the Gulf Coast. The optimal N_T value is 16-32 for many watersheds located in the Upper and Central Mississippi Valley, the Central Great Plains, and the Atlantic Coast. The optimal N_T value is between 64-90 for watersheds in the Upper and Central Great Plains, a few watersheds in the Mississippi Valley, and several watersheds in the Great Lakes region and the Atlantic Coast. The optimal N_T value is equal to 128 for only six watersheds, four of which are located in the Western USA. There is some spatial clustering of watersheds with a similar value of N_T which signifies that the optimal value of N_T is determined by the climatic properties and watershed characteristics.

Figure 3b shows the improvement in mean NSE obtained by increasing N_T from 1 to the optimal value. For most of the 57 test watersheds, the increase in mean NSE was less than 0.10 when N_T was increased from 1 to the respective optimal values (Figure 3b): approximately half of these watersheds exhibited an increase in NSE between 0.05 to 0.10. The improvement in NSE was 0.10-0.20 for the three watersheds located in the Western snow-dominated region, the three watersheds located in the Atlantic Coast region, and the one watershed located in the state of Texas. Three watersheds exhibited greater than 0.20 improvement in NSE. It must be noted that improvements in NSEs shown in Figure 2b are statistically significant.

Figure 3c shows the increase in mean NSE when N_T was increased from 1 to 128. These patterns are very similar to those in Figure 3b. One natural question that arises here is what improvement in NSE would be obtained if N_T is increased from optimal value to all the watersheds (128 in this case)? Figure 3d shows the increase in NSE obtained by increasing N_T from optimal value to 128 watersheds. In several watersheds, the NSEs decreased. Though not shown here, the decrease in

NSE was small in most watersheds. In most of the other watersheds, the increase in NSE was less than 0.05 which can be deemed negligible. There were only four watersheds where the increase was between 0.10 to 0.20, and two watersheds where the increase was greater than 0.20. These results convincingly show that the mean NSE values plateau after optimal N_T value in most watersheds.

In summary, the optimal N_T value is much smaller than 128 for most of the watersheds. The optimal value of N_T for a watershed is related to the climate in which the watershed is located. The optimal N_T value is also determined by the watershed characteristics. Increasing N_T value beyond the optimal results in a small and statistically insignificant increase in NSE which implies that an increase in NSE occurs due to improvement in predictions at a few time steps. In several watersheds, increasing N_T value beyond optimal may result in poorer performance.

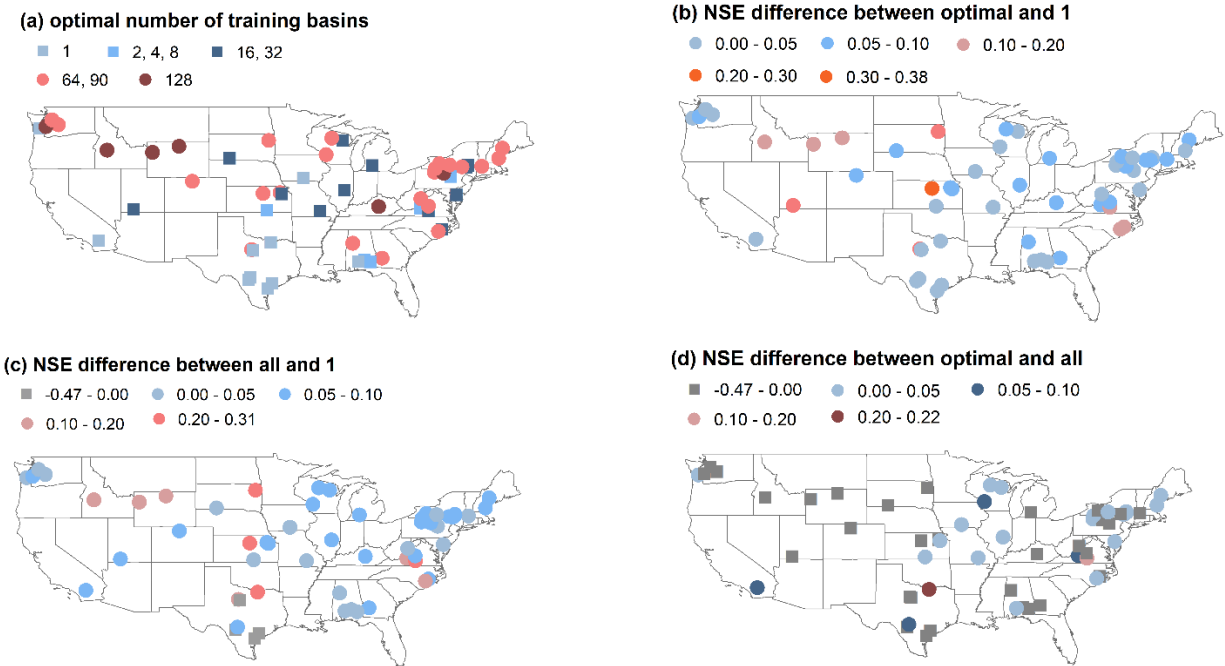


Figure 3. Experiment 1- Climatic statistics for watershed similarity. (a) The optimal number of training watersheds (N_T) corresponding to each of the 57 test watersheds. (b) Difference between the Nash-Sutcliffe Efficiencies (NSEs) obtained by using optimal N_T and $N_T = 1$. (c) Difference between NSEs obtained by using $N_T = 128$ and $N_T = 1$. (d) Difference between NSEs obtained by using $N_T = 128$ and optimal N_T .

Figure 4 compares the N_T values obtained in experiment 1 to the N_T values obtained in experiments 2 and 3. In experiments 2 and 3, statistic attributes and a combination of static and climatic attributes were used for selecting similar donor watersheds, respectively. The optimal N_T values obtained in experiment 2 were similar to the optimal values obtained in experiment 1 with small differences. There were, however, a few watersheds where N_T was quite different from that obtained in experiment 1: in most of these cases, N_T values obtained from experiment 2 were

higher. The optimal N_T values obtained in experiment 3 were smaller than those obtained in experiment 1 for many watersheds. These results indicate that the similarity measure used to select donor watersheds has some effect on the optimal N_T values.

Figure 5 compares the optimal NSE values obtained by experiments 1, 2, and 3 where optimal NSE refers to the NSE value obtained by using optimal N_T . The optimal NSEs obtained in all the experiments were similar when optimal NSEs obtained by experiment 1 were greater than 0.5. For some of the watersheds, the optimal NSEs obtained by the three experiments were quite different when the optimal NSEs obtained by experiment 1 were less than 0.5. It appears that using a combination of climatic and static attributes is the best method of selecting training watersheds in the sense that it results in optimal performance with smaller N_T .

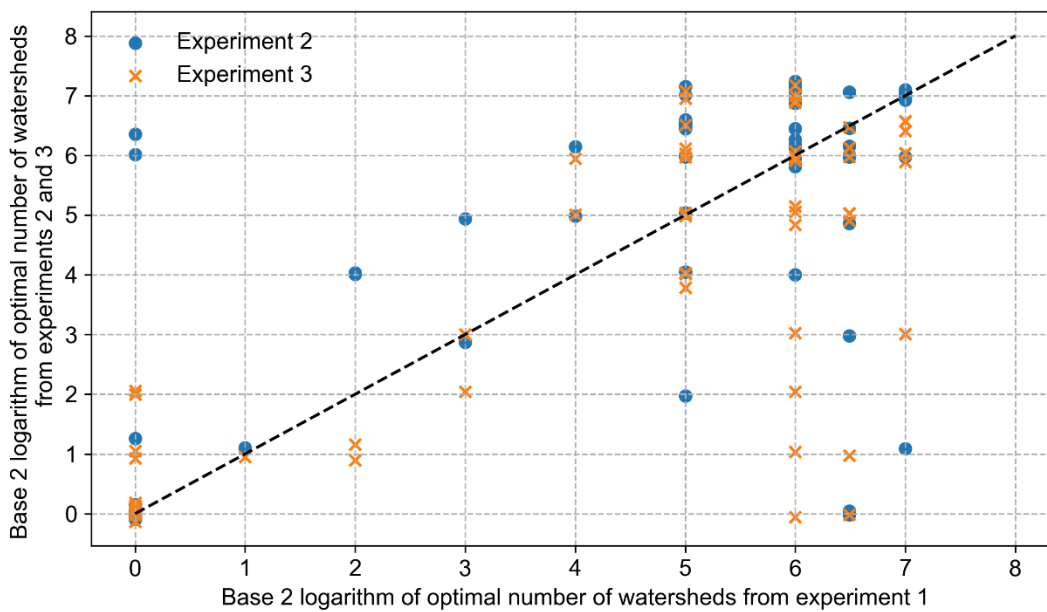


Figure 4. Comparison of the optimal number of watersheds (N_T) obtained from experiments 1, 2, and 3. A small Gaussian noise with a standard deviation of 0.1 has been added to the y-axis so that overlapping points become clearly visible.

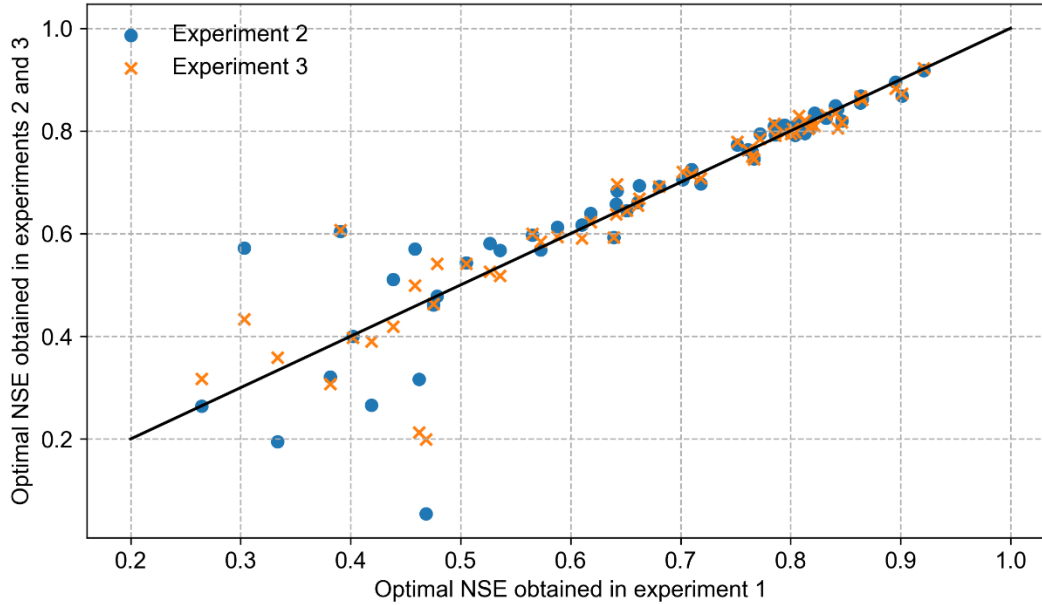


Figure 5. Comparison of optimal NSE values obtained from experiments 1, 2, and 3. Here, ‘optimal NSE’ refers to the NSE obtained by using the optimal number of training watersheds.

4.2 Experiments at ungauged locations

Figure 6a shows the optimal values of N_T for different watersheds across the USA obtained in experiment 4. There exists some spatial structure in the optimal N_T values, i.e., similar optimal N_T values were clustered together. The optimal N_T value was greater than 64 for several of the watersheds in the Atlantic Coast, the Eastern Great Lakes region, and the Mississippi Valley. The optimal N_T values were less than 32 for watersheds located in the Southern USA such as Texas, the Gulf Coast, Southern Utah, and Southern California.

Figure 6b shows the increase in NSE value when N_T is increased from 1 to its optimal value. A large increase in NSE (> 1) was observed in the Great Lakes region, the Atlantic coast, the Gulf Coast, the Northern Rocky Mountains, and the High Plains. Most of the watersheds in the arid Great Plains region exhibited only a small or moderate increase in NSE (< 1). Figure 6c shows the increase in NSE obtained when N_T is increase from 1 to 128. The patterns in Figure 6c are quite similar to the patterns in Figure 6b.

Figure 6d shows the increase in NSE when N_T was increased from optimal value to 128. In most of the watersheds, the increase in NSE was less than or equal to zero. Note that these also include the watersheds where optimal N_T was equal to maximal N_T , where the increase in NSE was 0. In most of the other watersheds, the increase in NSE was less than 0.05. These results indicate that the optimal N_T value is less than 128 in the ungauged scenario as well. Using the data from all the watersheds may result in a sub-optimally trained model.

The optimal N_T values were significantly greater in experiment 4 (ungauged location) compared to those in experiment 1 (gauged scenario) for some watersheds. Similarly, there were many

watersheds where the optimal N_T values obtained in experiment 4 were smaller than the optimal N_T values obtained in experiment 1. This is contrary to the intuition that more donor watersheds would be required to train an optimal LSTM model in the ungauged scenario. The reason for this intuition is that we expect that using more donor watersheds would compensate for at least some of the missing hydrological information contained in the parent watershed(s). The results, however, indicate that the hydrologic information contained in a parent watershed may or may not be obtainable from other watersheds depending upon the watershed's characteristics. This conclusion is further strengthened by Figure 7 which compares the optimal NSEs obtained in experiment 1 to the optimal NSEs obtained in experiments 4, 5, and 6. There were several test watersheds where the optimal NSE values obtained in experiments 4, 5, and 6 were significantly smaller than the NSEs obtained in experiment 1.

Particularly, when NSEs obtained in experiment 1 were smaller than 0.5, then NSEs obtained in the ungauged scenario were smaller than those obtained in experiment 1. When NSEs obtained in experiment 1 were greater than 0.5, then NSEs obtained in the ungauged scenario were close to or smaller than those obtained in experiment 1. Further, Figure 7 also indicates that using watershed static attributes is slightly more appropriate to define similarity measures as NSEs obtained in experiment 5 were better or equal to the NSEs obtained in experiment 4.

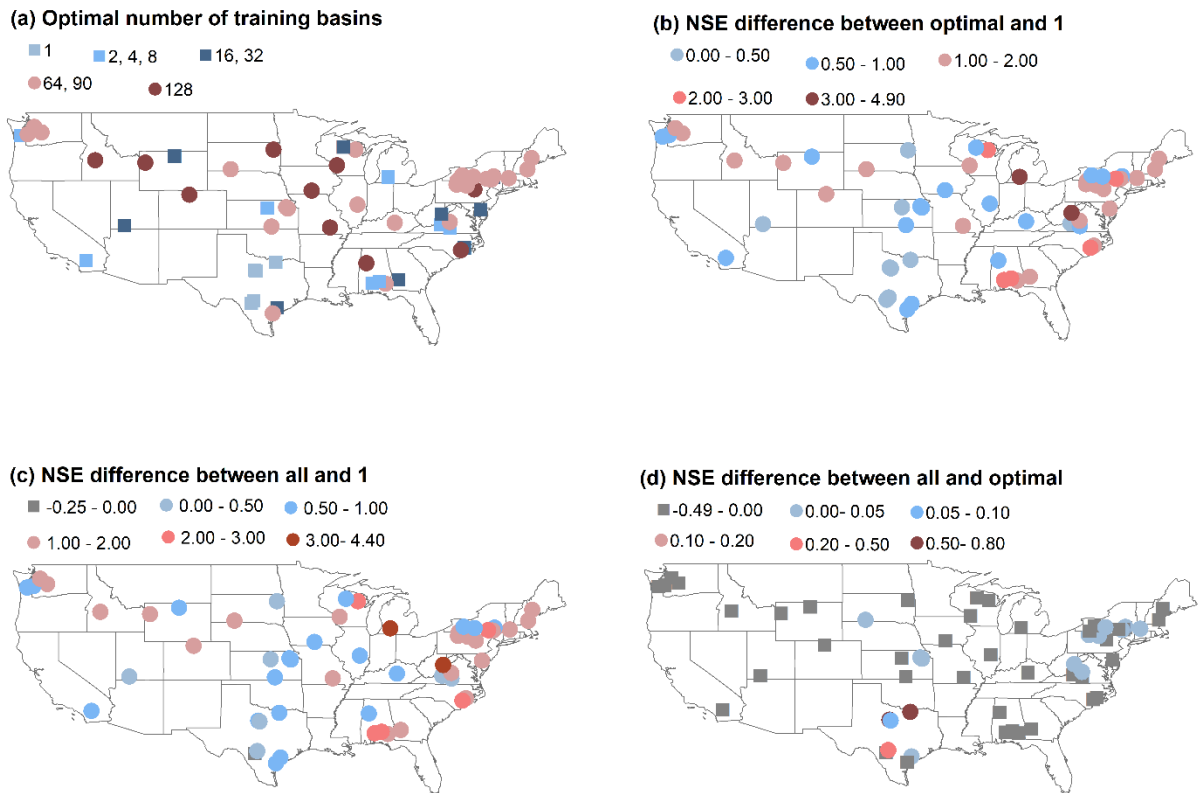


Figure 6. Experiment 4- Climatic statistics for watershed similarity. (a) The optimal number of training watersheds (N_T) corresponding to each of the 57 test watersheds. (b) Difference between the Nash-Sutcliffe

Efficiencies (NSEs) obtained by using optimal N_T and $N_T = 1$. (c) Difference between NSEs obtained by using $N_T = 128$ and $N_T = 1$. (d) Difference between NSEs obtained by using $N_T = 128$ and optimal N_T .

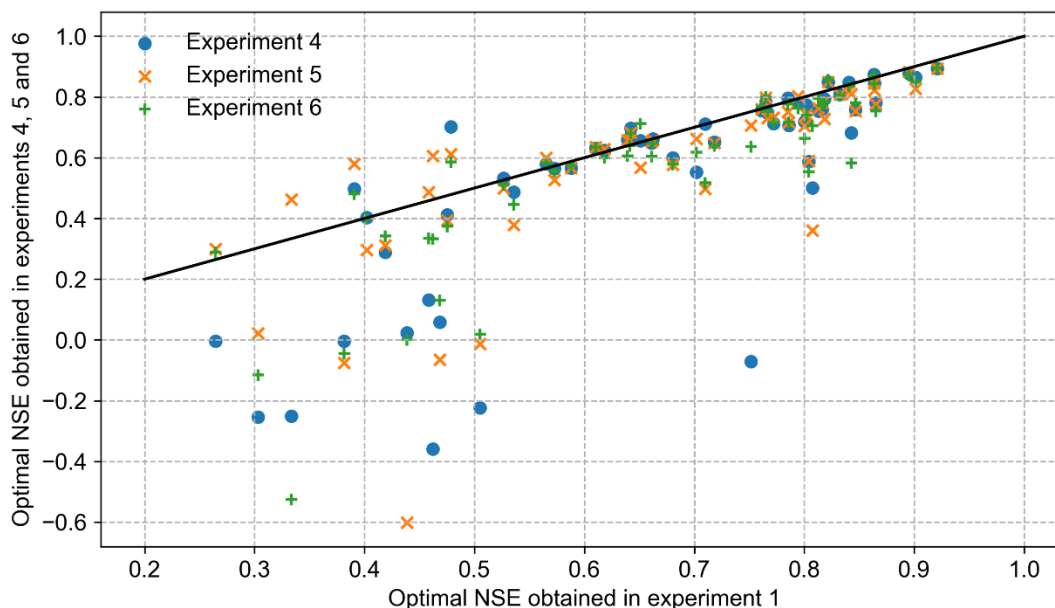


Figure 7. Comparison of optimal NSE values obtained from experiments 1, 4, 5, and 6. Here, ‘optimal NSE’ refers to the NSE obtained by using the optimal number of training watersheds.

4.3 Analysis at monthly timescales

Figure 8 (a-f) compares the optimal N_T values for streamflow prediction at monthly and daily timescales. For the majority of the 57 watersheds, optimal N_T values obtained for monthly timescale predictions were equal to or smaller than those obtained for daily timescale predictions. Still, there were some watersheds for which optimal N_T values for monthly timescale were smaller than those obtained for daily timescale. Overall, it can be concluded that using data using several watersheds improves streamflow prediction accuracy at monthly timescale also.

Figure 8 (g, h) show the increase cumulative distribution function of increase in NSE values as N_T is increased from 1 to the optimal value. In experiments 1, 2, and 3 (Figure 8g), the increase in NSE was less than 0.10 for about 85, 80, and 75% of the watersheds, respectively. In experiments 4, 5 and 6, the NSEs increased significantly since the watershed are assumed (hypothetically) ungauged in these experiments. The increase in NSE was typically greater when a combination of climatic statistics and watershed attributes (experiments 3 and 6) were used for selecting donor watersheds.

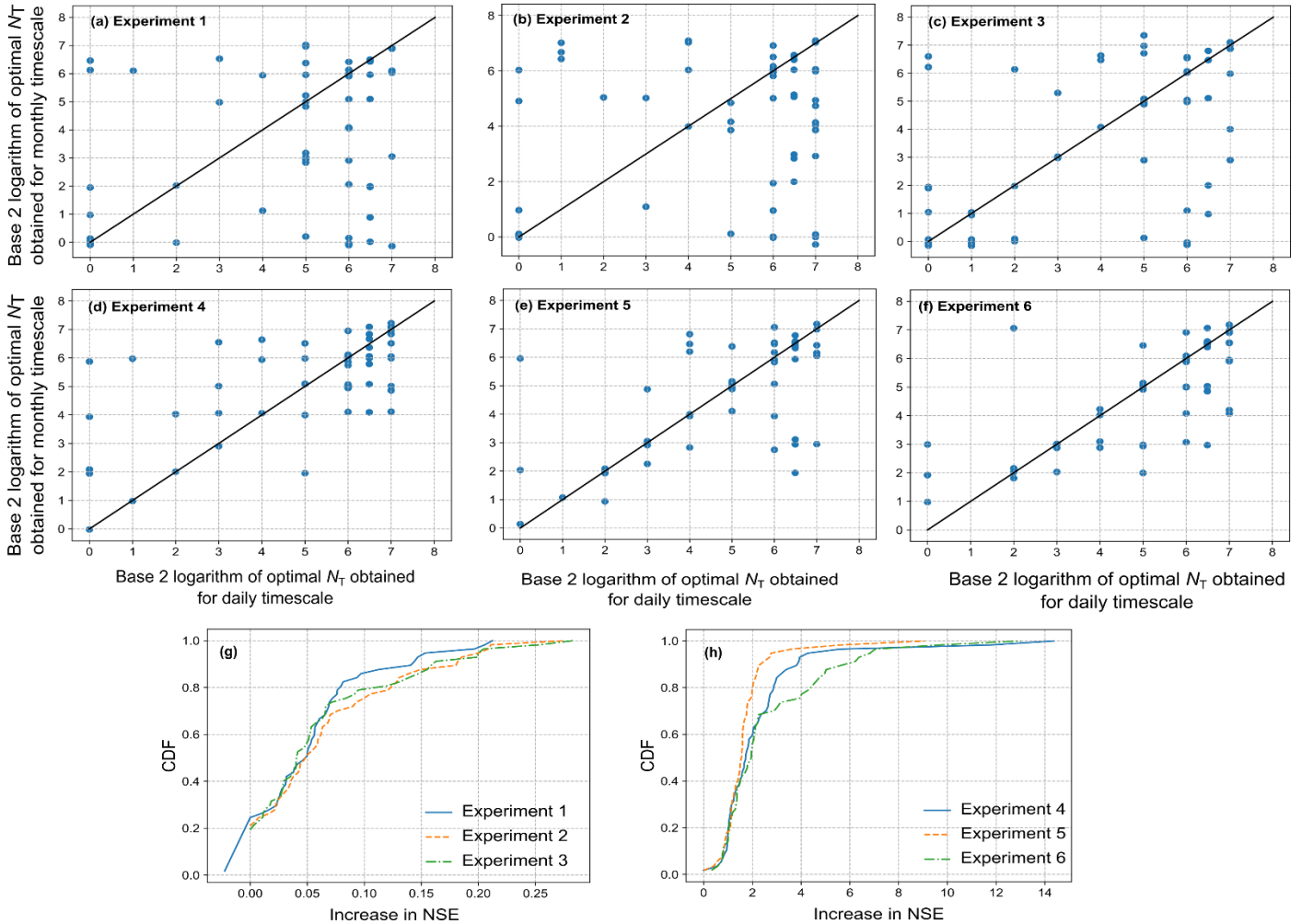


Figure 8. (a-f) Comparison of optimal number of training watersheds (N_T) obtained for streamflow predictions at daily (on x-axis) and monthly (on y-axis) timescales. (g, h) CDF of increase in NSE as N_T is increased from 1 to the optimal value.

5. Discussions

5.1. Why are the NSEs obtained by the two models statistically indistinguishable?

It must be noted that the optimal N_T value means that NSE obtained by using these many training watersheds (selected using a particular similarity measure) is statistically indistinguishable from the NSE obtained by using larger N_T values. The NSEs obtained by the two models are statistically indistinguishable if the difference in performance occurs only at a few time steps. Figure 9 illustrates this phenomenon, which compares the predicted streamflow values obtained by the two LSTM models: (1) the one that yielded maximum NSE (on the x-axis; referred to as the maximum model in what follows) and (2) the one trained using optimal N_T (on the y-axis; referred to as optimal model). The four subplots correspond to the four different watersheds in cluster 0. The streamflows predicted by the two models are quite similar for all four watersheds even though the

difference between the training watersheds for the optimal model and maximum model were very different. The significant difference between the streamflow values obtained by the two models occurred only at a few time steps which makes the difference between the NSEs obtained by the two models statistically insignificant. Similar results were obtained for the remaining test watersheds (not shown).

It is possible that if a longer streamflow time series were used for testing purposes, statistically indistinguishable NSE differences could have become statistically distinguishable. Also, it is plausible that if more than 434 watersheds were used, NSE could have improved statistically significantly. It seems unlikely, however, since, for the majority of the 57 test watersheds, the NSE values started to saturate when N_T was increased beyond the optimal value. Note that earlier studies that have claimed that using more and more data increases streamflow prediction accuracy did not take into account uncertainty in NSE values which is important when comparing two models (Clark et al., 2021).

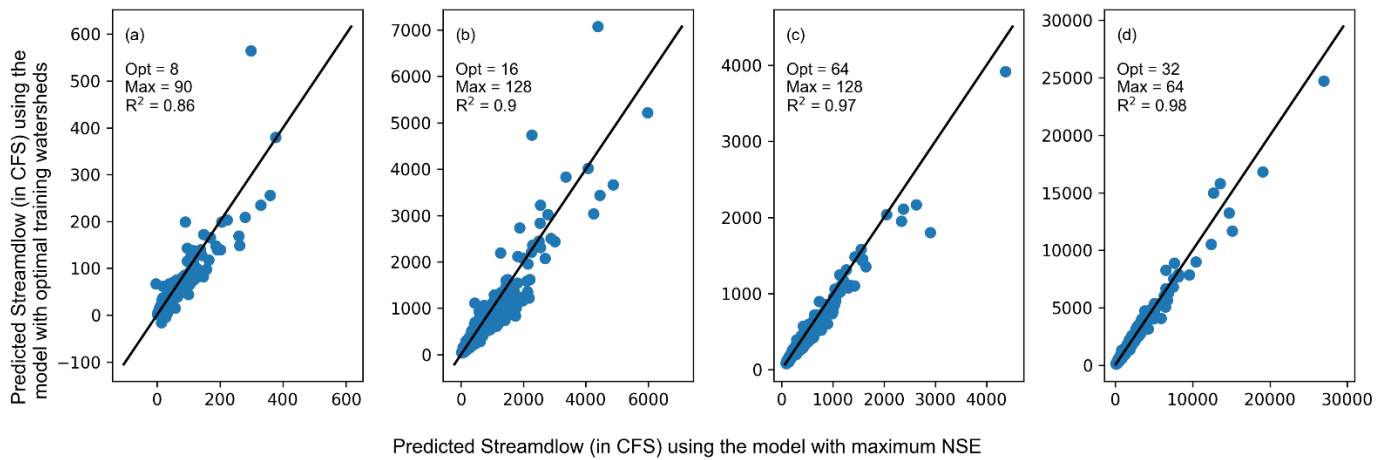


Figure 9. Comparison of predicted streamflow obtained by the LSTM model that yielded maximum NSE (x-axis) and predicted streamflow obtained by the LSTM model with optimal training watersheds (N_T). Legend: ‘Opt’ denotes the optimal N_T , ‘Max’ denotes the number of training watersheds used for the LSTM model that yielded maximum NSE, and R^2 denotes coefficient of determination. The four subplots correspond to four different watersheds in cluster 0.

The areal average rainfall and streamflow time series contain measurement errors (Moulin et al., 2009; Renard et al., 2011; Kiang et al., 2018). Errors in areal average rainfall also occur due to a lack of rain gauges to capture spatial variability in rainfall (Moulin et al., 2009). These errors may be especially severe during peak events (Bardossy and Anwar, 2022; preprint). It is likely that these errors start to dominate the learning process when N_T value is increased beyond the optimal value, i.e., the variance of the hydrologically relevant phenomenon becomes smaller than the variance of the errors. In summary, even if the additional donor watersheds contain relevant

hydrological information, LSTMs may not be able to extract this information due to errors in the data.

There was some spatial structure in N_T values in all six experiments. Typically, watersheds with spatial proximity have similar climatic statistics and similar watershed characteristics. This implies that watersheds with similar dynamics and static attributes tend to have similar values of optimal N_T . Small N_T values were observed in arid regions such as Texas, California, and the Gulf Coast region. High N_T values were observed in humid regions such as the Great Lakes region, the Atlantic Coast region, and the Pacific Northwest. High N_T values were also observed in the western snow-dominated region. In several of the 57 test watersheds, increasing N_T beyond the optimal value resulted in smaller NSE – the difference was statistically insignificant, however, in most cases. The decrease in NSE might be because of higher measurement noise compared to the increase in the hydrologically relevant information as more and more donor watersheds are added to train the LSTMs.

5.2. What part of streamflow time series improves as the LSTM is trained using more data?

It is possible that using data from more donor watersheds for training improves only some parts of the streamflow time series (such as peak events) while other parts are not improved. To answer this question, we divided a streamflow time series into three parts (following Krueger et al., 2009): driven-fast, driven-slow, and non-driven. The driven fast part was defined as part of the streamflow that occurred during the days when precipitation was greater than 0.1 mm: it typically consists of rising limbs of streamflow hydrographs. The driven-slow part was defined as part of the streamflow time series during the days when precipitation was below 0.1 mm, and the streamflow value was 30 percentile value: it consists of the initial phase of the recession limb of the hydrograph. The remaining part of the streamflow hydrograph was defined as non-driven.

We found that typically, the prediction of all three parts of a streamflow time series improved as the number of donor watersheds increased. But there were no systematic patterns. A few watersheds, however, did show some systematic patterns. Typically, very low and very high flows were poorly predicted by the LSTM models, irrespective of the number of training watersheds used. The predictions of these extreme flows did improve for the high flows. But to improve the high flows, the LSTM models seem to have become too sensitive to rainfall. To elaborate on this point, Figure 10 shows the observed and predicted streamflow hydrographs for a watershed (stream gauge number 08164600) belonging to cluster 5. The predicted hydrographs are the ones obtained by the LSTM models trained with $N_T = 1$ and $N_T = 64$. The optimal N_T in this watershed is 1 and the maximum NSE was obtained by using $N_T = 64$.

In Figures 10a, 10c, and 10d, the model with $N_T = 1$ underpredicts the streamflow peaks while the model with $N_T = 64$ predicts the peaks relatively accurately. In Figures 10b and 10e, the model with $N_T = 64$, significantly overpredicts the peaks, while the model with $N_T = 1$ predicts the peaks relatively accurately. This illustrates that the model $N_T = 64$ might have become over

sensitive to rainfall. Other possibility is that the model with $N_T = 64$ captures the rainfall-runoff dynamic but the rainfall events corresponding to the Figures 10b and 10e were erroneous.

Similarly, for a few watersheds, the extremely low flows were consistently overpredicted by the models with larger N_T . This is illustrated in Figure 11, which compares the logarithm of observed and predicted streamflow values for a watershed belonging to cluster 2 (stream gauge number 01181000). The predicted streamflows are the ones obtained by $N_T = 1$ and $N_T = 64$. Clearly, the low flows were overpredicted by the model with $N_T = 64$, while the degree of overprediction was smaller by the model with $N_T = 1$. Overall, however, the model with $N_T = 64$ predicted streamflow more accurately. Further, in several watersheds, extremely low flows were poorly predicted by a model irrespective of the N_T value. It is possible that giving more weightage to low flows increases the prediction accuracy of these flows.

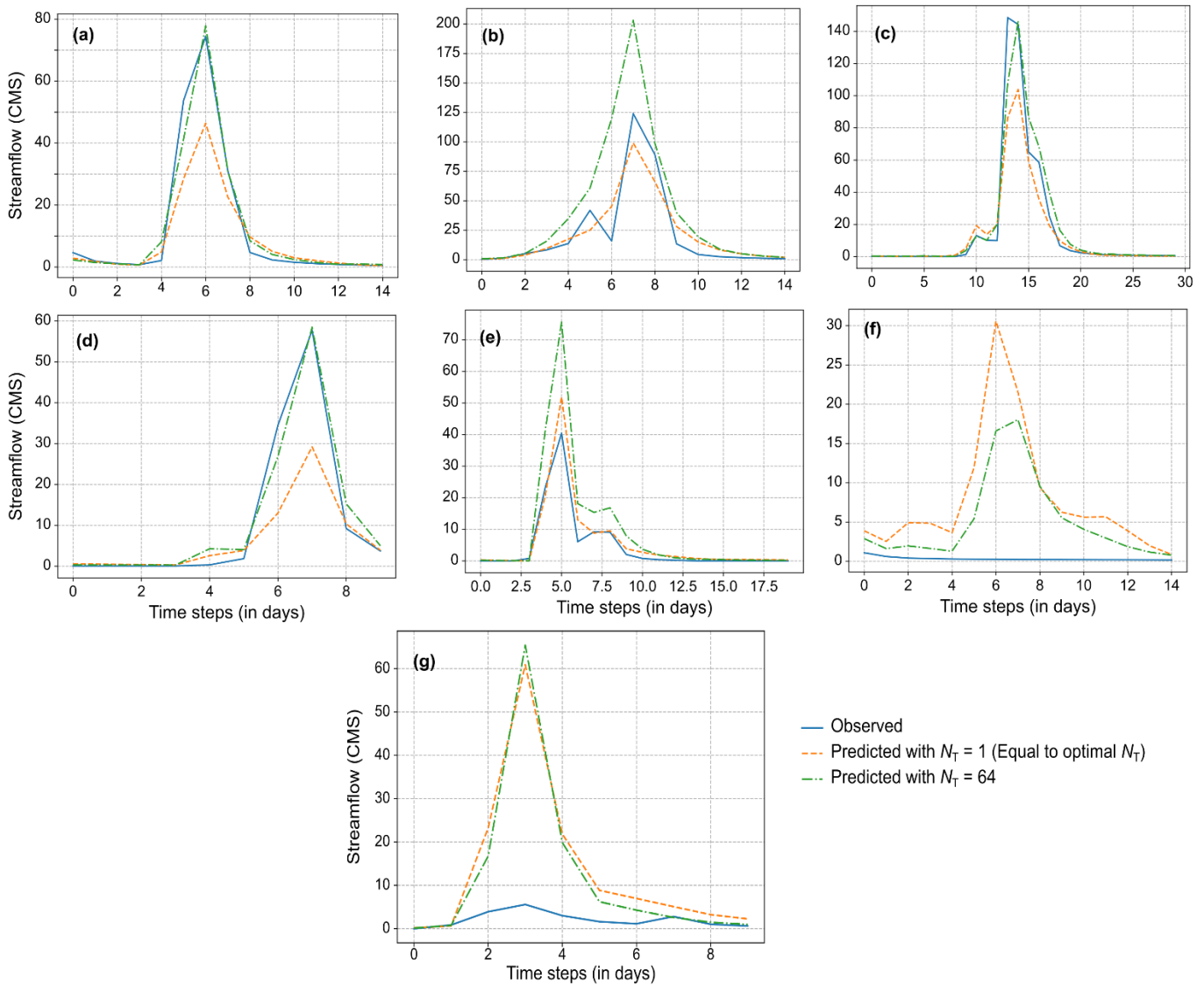


Figure 10. Observed and predicted streamflow hydrographs obtained by using LSTM models trained with $N_T = 1$ and $N_T = 64$. The CAMELS stream gauge number for this basin is

08164600. The optimal N_T was equal to 1 for this watershed, and maximum NSE was obtained with $N_T = 64$. The predicted hydrographs shown in this plot are the ones obtained in experiment 1 where donor watersheds were selected based on similarity of climatic statistics.

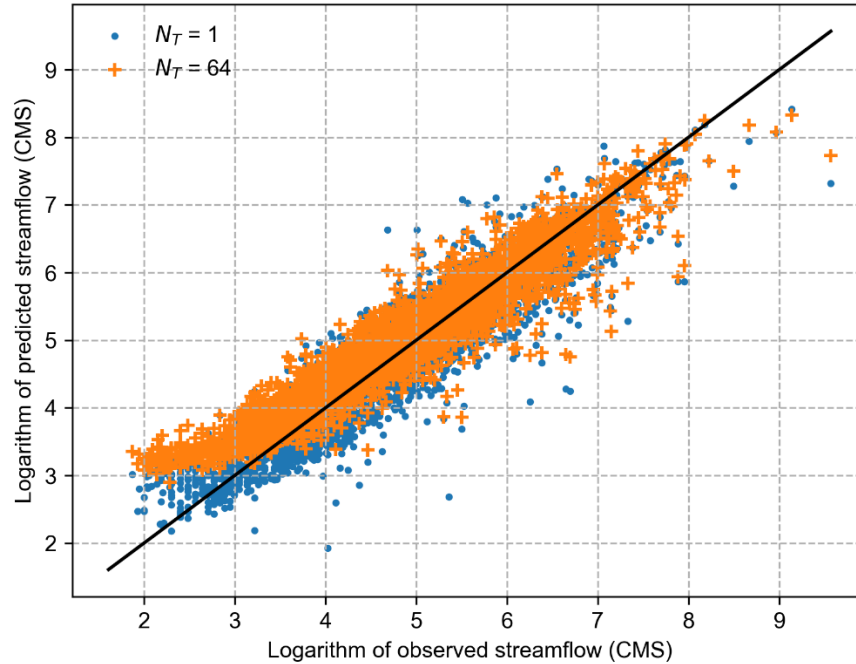


Figure 11. Logarithm of the observed and predicted streamflow. Blue dots represent the streamflow predicted by the LSTM model with $N_T = 1$, and orange '+' represent the streamflow predicted by the LSTM model with $N_T = 64$. The optimal N_T for this watershed was 64. The N_T that yielded maximum NSE was also 64. The gauge number of this watershed is stream gauge number 01181000 and it belongs to cluster 2.

5.3. Is selecting donor watersheds using a systematic similarity measure useful?

To analyze the importance of similarity measures used to select donor watersheds for training, a small experiment was conducted. In this experiment, 7 watersheds were selected from the 57 test watersheds belonging to 7 different clusters (see Figure 1 for clusters). For each of the watersheds, experiment 1 was repeated, but the donor watersheds were selected randomly. The number of random donor watersheds selected was the same as the optimal number of donor watersheds obtained in experiment 1. The donor watersheds were selected with 25 different random seeds. Thus, 25 different LSTM models with 25 different sets of donor watersheds were obtained. Each of the 25 models was an average of 4 models obtained using 4 random seeds. Figure 12 shows the boxplots of NSE values obtained in this experiment along with optimal NSE values obtained in experiment 1. Optimal NSEs obtained in experiment 1 were typically higher than the NSEs obtained when donor watersheds were selected randomly. This result clearly illustrates the importance of using a systematic similarity measure for selecting donor watersheds. The

hydrologic information contained in N nearest (according to climatic statistics) watersheds is typically more than the information contained in N randomly selected watersheds.

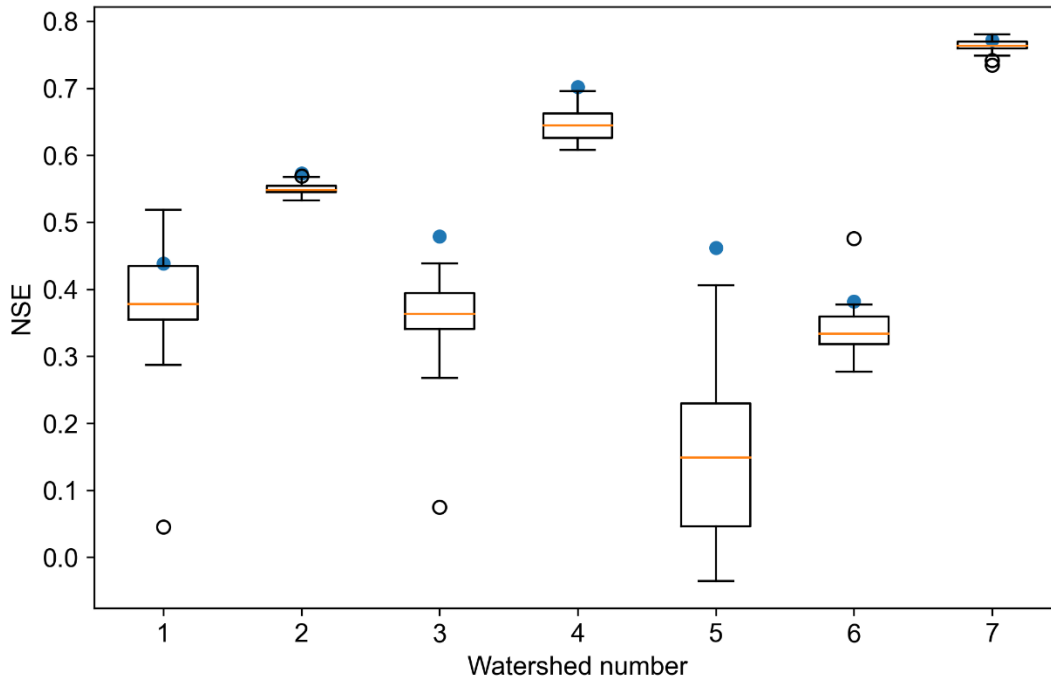


Figure 12. Boxplots of NSEs obtained by using randomly selected donor watersheds equal in number to optimal training donor watersheds obtained in experiment 1, along with optimal NSEs obtained in experiment 1 (blue dots).

5.4. Why are optimal N_T values were typically smaller than 128?

All 6 experiments showed that optimal N_T values were much smaller than 128 for most watersheds. These results contradict other studies that claim that the performance of LSTMs continues to improve as more and more data are used to train the model. There were only a few watersheds for which the optimal N_T was 128. There could be two reasons for the smaller value of optimal N_T : (1) using more training watersheds beyond optimal N_T does not *add* any *extra* information to be learned by the LSTM, and/or (2) watersheds selected beyond optimal N_T do not *contain* any information relevant to rainfall-runoff dynamics of the parent watershed.

Reason 1 applies to some watersheds whereas reason 2 applies to some other watersheds. This is evident from Figure 13 which compares the optimal N_T values obtained from experiments 1 and 4. The color of a point in the figure represents the difference in NSEs obtained in experiment 1 and experiment 4. Note that the models trained in experiment 1 had access to training data from parent watersheds while the models trained in experiment 4 did not have access to training data from parent watersheds. For several watersheds, N_T values obtained in experiment 4 were greater than N_T values obtained in experiment 1; the NSE difference was positive for some of these

watersheds and negative for other watersheds. These are the watersheds for which some of the hydrologic information contained in parent watersheds could be obtained from additional donor watersheds. Here, the term ‘additional donor watersheds’ refers to the donor watersheds beyond the optimal as obtained in experiment 1.

For some watersheds, N_T values obtained in experiment 4 were equal to those obtained in experiment 1 (points that fall on the 1:1 line); the NSE difference was positive for some of these watersheds and negative for other watersheds. This indicates that additional donor watersheds could not compensate for the information missing from the parent watersheds. Among these watersheds the ones for which NSE differences were negative, it can be concluded that donor watersheds contained as much information about streamflow dynamics as the parent watershed. The watersheds for which NSE differences were positive, it can be concluded that donor watersheds did not contain as much information about streamflow dynamics as the parent watershed.

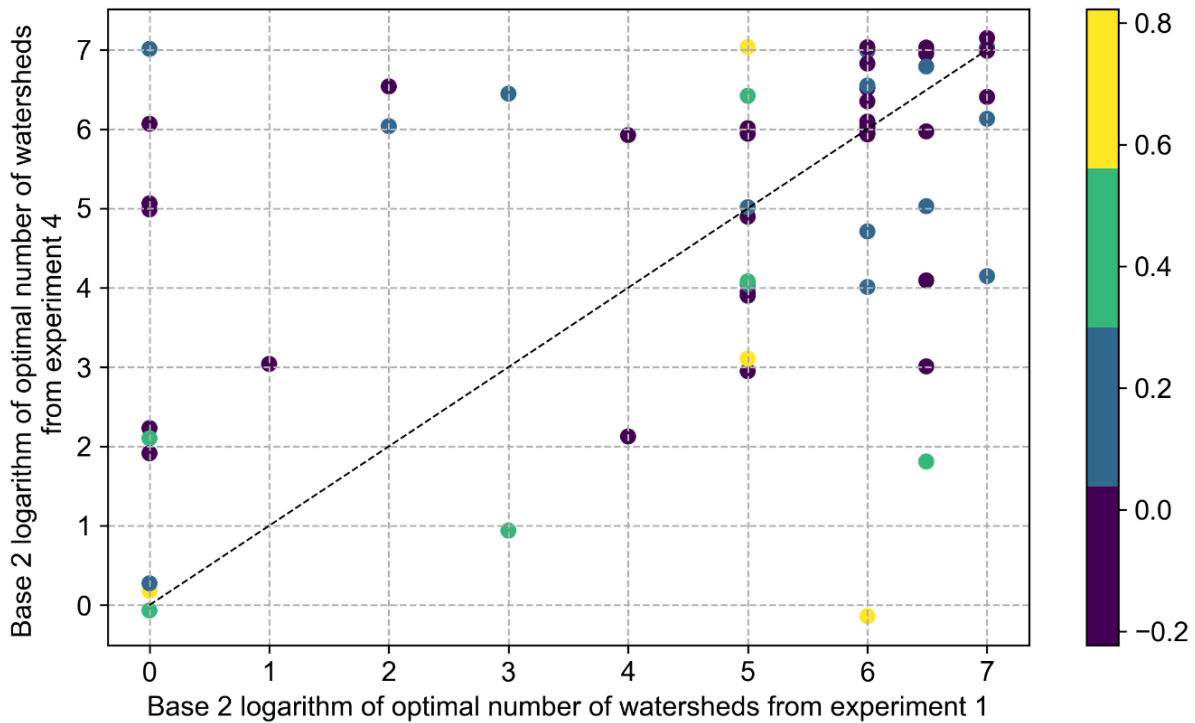


Figure 13. Comparison of the optimal number of training watersheds (N_T) obtained from experiments 1 and 4. The color of a dot represents the difference in NSEs obtained by experiment 1 and experiment 4. Positive NSE difference means that NSE obtained in experiment 1 was greater than that obtained in experiment 4. A small Gaussian noise with a standard deviation of 0.1 has been added to the y-axis so that overlapping points become clearly visible.

For many watersheds, N_T values obtained in experiment 4 were smaller than those obtained in experiment 1; the NSE difference was positive for most of these watersheds. This implies that the

donor watersheds contained only a small amount of information necessary to capture streamflow dynamics in the parent watersheds.

Figure 14 shows the categorization of the 57 test watersheds based upon the optimal N_T s and optimal NSEs obtained in experiments 1 and 4. This categorization can be referred to as *donor information categorization* as it tells us about the hydrological information contained in donor watersheds. In what follows, we denote by N_1 and N_2 the optimal N_T s obtained in experiments 1 and 4, respectively. We denote by NSE_d the difference between optimal NSEs obtained in experiments 1 and 4. A positive value of NSE_d for a given watershed means that the NSE obtained in experiment 1 was greater than the NSE obtained in experiment 4 for the watershed. The 57 test watersheds have been divided into nine categories. The categories 1, 2, and 3 contain watersheds for which $N_1 < N_2$. As discussed above, for these watersheds, at least some of the information contained in parent watersheds could be obtained from additional donor watersheds. Most of these watersheds are located in a contiguous region overlapping the Mississippi Valley, the Great Plains, and the Gulf Coast. A cluster of these watersheds was also located in the eastern Great Lakes region.

Categories 4, 5, and 6 contain watersheds for which $N_1 = N_2$, and additional donor watersheds could not supply any relevant information. Categories 4 and 5 contain the watersheds for which NSE_d was negative or slightly greater than zero. For these watersheds, donor watersheds (not additional) contained approximately the same hydrological information as the parent watersheds. These watersheds are contained in the Atlantic Coast, the eastern Great Lakes region, and the Northern Rocky Mountains. These are the watersheds where streamflow dynamics can be captured even if the data from parent watersheds is not available. Category 6 contains the watersheds for which NSE_d was greater than 0.2. These are the watersheds where information contained in donor watersheds was not enough to compensate for the information contained in the parent watershed. All these watersheds are located in the state of Texas.

Category 7 contains the watershed for which $N_1 > N_2$ and $NSE_d < 0$. These are only two watersheds in this category located in the Atlantic Coast and the Great Lakes region. Categories 8 and 9 contain watersheds for which the information contained in the parent watersheds is necessary to capture rainfall-runoff dynamics. These watersheds are mostly located in the Atlantic Coast, the Great Lakes region, the Ohio Valley, the Tennessee Valley, and the eastern Gulf Coast. Some of these watersheds are also located in Northern Texas, the Great Plains, the High Plains, the Southern Rocky Mountains, and the Pacific Northwest.

Figure 14 also shows that there is some spatial structure in information categorization in the Eastern USA. The spatial structure is quite significant in the Mississippi valley, the Ohio Valley, the Tennessee valley, and Southern Atlantic region. In the Western USA, the spatial structure does seem to exist. It is possible that the spatial structure in the Western USA is not visible due to fewer watersheds in this region.

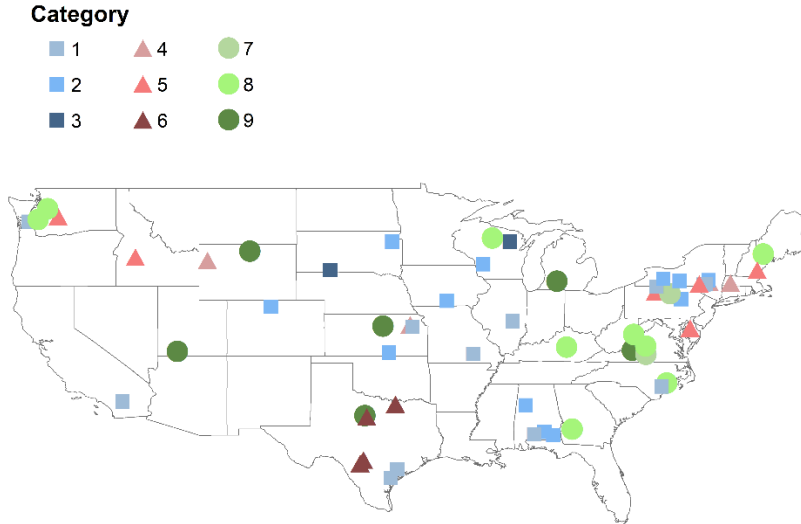


Figure 14. Categorization of watersheds based upon the optimal number of training watersheds (N_T) and optimal NSE obtained in experiment 1 (gauged scenario) and experiment 2 (ungauged scenario). Denote by N_1 and N_2 the optimal N_T obtained in experiments 1 and 2, respectively, and by NSE_d the difference between optimal NSEs obtained by experiment 1 and experiment 2. Category 1 (**C1**): $N_1 < N_2, NSE_d \leq 0$; **C2**: $N_1 < N_2, NSE_d \in (0,0.2)$; **C3**: $N_1 < N_2, NSE_d \geq 0.2$; **C4**: $N_1 = N_2, NSE_d \leq 0$; **C5**: $N_1 = N_2, NSE_d \in (0,0.2)$; **C6**: $N_1 = N_2, NSE_d \geq 0.2$; **C7**: $N_1 > N_2, NSE_d \leq 0$; **C8**: $N_1 > N_2, NSE_d \in (0,0.2)$; **C9**: $N_1 > N_2, NSE_d \geq 0.2$.

These results also shed some light on the uniqueness of place argument (Beven, 2000; Beven, 2020; Nearing et al., 2021) which asserts that each watershed is hydrologically unique. While this certainly seems to be true in the sense that individual hydrologic flow paths and their flow characteristics may indeed be unique. It seems that the uniqueness of place defined in this sense does not necessarily imply unique rainfall-runoff dynamics. Specifically, Figures 7, 13, and 14 collectively show that there were several watersheds where (overall) streamflow dynamics could be learned using the data only from donor watersheds, i.e., donor watersheds contain similar hydrological information as the parent watersheds. There were other watersheds where streamflow dynamics could not be learned using the data from only the donor watersheds as well as it could be learned using the data from the parent watershed; it can be concluded that these are the watershed with unique rainfall-runoff dynamics.

5.5. Limitations of the study

The 57 test watersheds in this study were selected based on the change in the contribution of the high-frequency component to streamflow variance over the study period. This change was related to the change in rainfall and temperature statistics by Gupta et al., (2022). But it is likely that there were other physical changes in the watersheds such as changes in vegetation structure which may be responsible for the change in the statistical structure of streamflow. Further, it is difficult to say whether the rainfall-runoff responses in these watersheds have changed. The key point is that the

statistical structure of streamflow has changed in these 57 test watersheds due to climate change, but the rainfall-runoff response may not have changed. Thus, the effect of climate change on watershed hydrology can only be considered limited in these 57 test watersheds. This is a limitation of the study. Nevertheless, the results presented in this study illustrate that the data from donor watersheds can be used to extract hydrologically relevant information for a watershed where streamflow statistical structure has changed between training and test periods. We believe that these results are also valid for the watersheds where streamflow statistical structure has not changed.

Another limitation of the study is that the several different strategies can be used to select the donor watersheds. In this study, only three general approaches were used. There exists a vast literature on hydrological similarity (see Wagener et al., 2007 for a review). Particularly, Li et al. (2022) showed that watersheds located (geographically) far away from the parent watershed may also contribute to capturing the rainfall-runoff dynamics in the parent watershed. But we note that for experiments 1, 2, and 3, we also trained an LSTM model with all the 434 watersheds. In these experiments, the optimal number of watersheds were below 434 as discussed above. Therefore, it can be concluded that the results presented in this study are robust.

Finally, we remark that the size of LSTM hidden layer used in this study was 256 (see also Kratzert et al., 2019c), which was tuned for the LSTM model trained using data from all the 434 watersheds. This parameter (size of hidden layers) was not tuned for LSTMs trained using data from smaller number of watersheds. Similarly, other hyperparameters such as sequence length (365 for all the models in this study) were not tuned separately for each of the LSTM models. Therefore, it is possible that tuning this parameter separately for each of the LSTM models will result in a better performance than reported here. This, if true, will only strengthen our conclusions. The author's experience is that separately tuning hyperparameters for each LSTM is computationally very expensive. These issues remain to be explored.

However, for a preliminary testing of this issue, we repeated the experiment-1 with hyperparameters for the 13 test watersheds belonging to cluster 2 (see Figure 1 for cluster labeling). Figure 15 compares the NSEs obtained by the LSTM models trained with 64 donor watersheds but by using different sets of hyperparameters. The number of neurons in the LSTM layer used in this study are 256. Figure 15 shows that even if we had used 125 or 312 neurons in the LSTM layer, the NSEs obtained would have been the same. Similarly, we used a minibatch size of 256 in this study. Figure 15 shows using a minibatch size of 32 would have yielded the same results. Using very small number of hidden neurons (=5) in the LSTM layer significantly degraded the NSE value. Thus, this investigation gives us further confidence that the hyperparameters used in this study are appropriate and the results and conclusions presented in this study are robust.

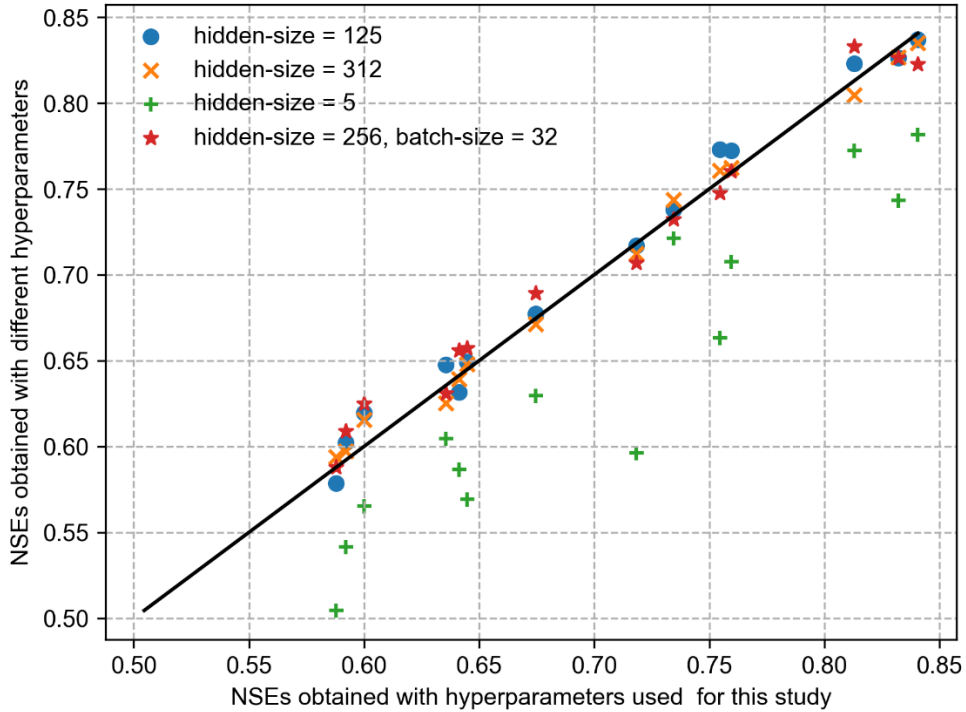


Figure 15. NSEs obtained by LSTM models with hyperparameter used in this study (on x-axis) and different hyperparameters (on y-axis). See the text for the hyperparameters used in this study. These results correspond to experiment-1 where donor watersheds were selected based on the similarity in climatic space. Further, these results correspond to the LSTM models trained with 64 training watersheds.

6. Summary and conclusions

The goal of this study was to assess the hydrologic information content in parent and donor watersheds. This was accomplished by using LSTMs as information extraction machines. Several LSTM models were trained using data from n watersheds where n was varied between 1 and 128. Two types of experiments were carried out where parent watersheds were either used or not used for training the LSTMs. The time period of the training data was fixed to 1980-1989. A total of 434 watersheds across the USA were used to train the models. The n training watersheds were selected based on the similarity of parent watersheds and donor watersheds. Three different similarity measures were used in this study: based on climatic statistics, based on static attributes, and based upon a combination of climatic statistics and static attributes. The following conclusions can be drawn from this study:

- (1) For both gauged and ungauged scenarios, optimal values of N_T were much smaller than 128 for most of the watersheds. LSTMs could not extract any (or could extract only a small amount of) hydrologically relevant information by increasing N_T beyond the optimal value.
- (2) Optimal value of N_T depended upon the similarity measure used to select donor watersheds. The effect of the similarity measure was significant only for a few watersheds. If one aims

to use as few donor watersheds as possible for practical convenience, it is recommended to use a combination of climatic statistics and static attributes as the similarity measure.

- (3) Optimal NSE values depended upon the similarity measure used to select the donor watersheds but only for the watersheds where the LSTMs were unable to extract much information about the rainfall-runoff dynamics (NSE was small). For other watersheds, the optimal NSEs obtained in experiments 1, 2, and 3 were quite similar.
- (4) Optimal NSEs obtained in the ungauged scenario were smaller than those obtained in the gauged scenario in several watersheds. There were other watersheds where the optimal NSEs obtained in the two scenarios were similar.
- (5) In several of the watersheds, the NSE values obtained using either 128 or 434 watersheds were smaller than the optimal NSE values. The decrease was small, however. We also hypothesized that this decrease in NSE might be due to the increasing influence of noise in data compared to the hydrological information as the data from more and more donor watersheds are used. Overall, it appears that one can train an LSTM model with all the watersheds available at the cost of misidentifying some noise as a hydrologic signal and a slightly smaller NSE.
- (6) In a few watersheds, increasing N_T seems to have resulted in excessive sensitive of the LSTM model to rainfall. Similarly, LSTM model with high N_T may also result in consistent underprediction of extremely low flows. Therefore, some caution is needed in using data from donor watersheds to train the LSTM models.

By comparing optimal N_T and optimal NSE between gauged and ungauged scenarios, the watersheds were categorized in terms of donor watershed information. This was referred to as donor information categorization. There was a significant spatial structure in the donor information categorization. This categorization tells us in which region of the USA we can expect to extract hydrologically relevant information from donor watersheds. This is especially relevant for prediction under climate change where we can expect that information contained in parent watershed(s) may become less useful.

The idea prevalent in recent literature is that one needs data from hundreds of donor watersheds to train an optimal LSTM model: as more and more data are used, the NSE would increase. The main conclusion of this study is that it is not so. Beyond an optimal value, the model accuracy does not improve significantly – improvement occurs only at a few time steps which results in statistically insignificant improvement.

Appendix:

Table A1. List of static attributes used in the study

Mean precipitation
Mean potential evapotranspiration
Precipitation seasonality

Fraction of snow
Aridity
High precipitation frequency
High precipitation duration
Low precipitation frequency
Low precipitation duration
Fraction of forest
Maximum monthly means of leaf area index
Difference between maximum and minimum monthly means of leaf area index
Maximum monthly mean of green vegetation fraction
Difference between maximum and minimum monthly means of green vegetation fraction
Mean elevation
Mean slope
Drainage area
Depth to bedrock
Soil depth
Soil porosity
Soil hydraulic conductivity
Maximum soil water content
Sand fraction
Silt fraction
Carbonate rock fraction
Geological permeability

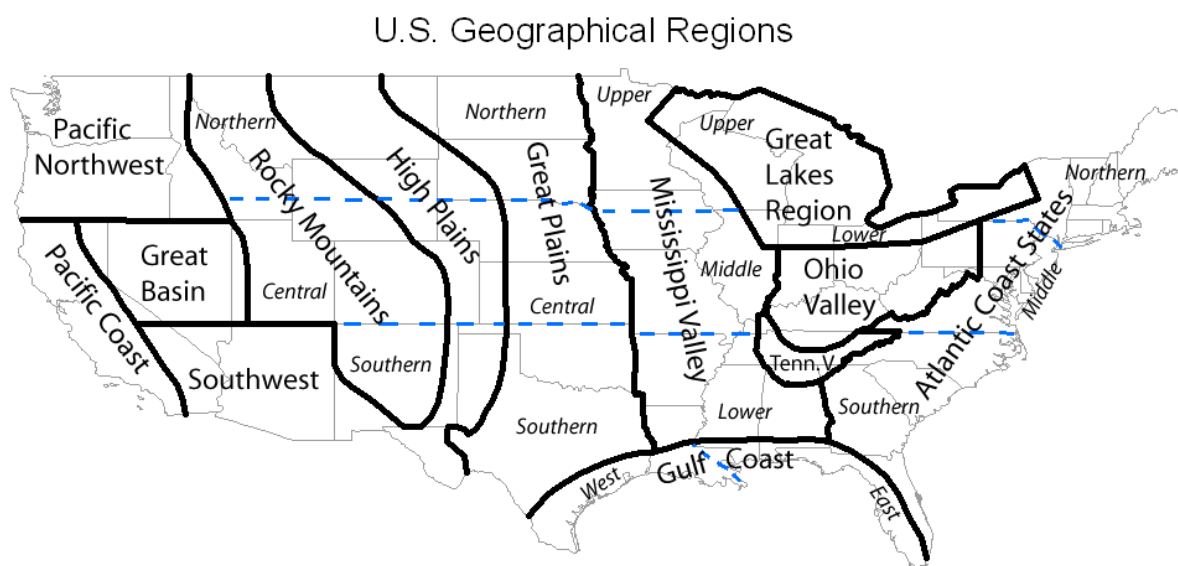


Figure A1. Map of the geographical regions referred to in this study. The details of this map can be found at National Oceanic and Atmospheric Administration (NOAA) through the link <https://www.ncdc.noaa.gov/temp-and-precip/drought/nadm/geography>

Acknowledgements

I would like to thank Ankit Ghanghas for providing an informal review of a earlier version of this paper. I am grateful to Rosemary Carroll, Patrick Sawyer, Chris Pearson, and Sean McKenna for helpful suggestions to improve the paper. The author was supported by the Maki Postdoctoral Fellowship during the performance of this work and preparation of the manuscript.

Funding

This work did not receive any funding from any external agency.

References

- Addor, N., Newman, A. J., Mizukami, N., & Clark, M. P. (2017a). The CAMELS data set: catchment attributes and meteorology for large-sample studies. *Hydrology and Earth System Sciences*, 21(10), 5293-5313.
- Addor, N., Newman, A. J., Mizukami, N., & Clark, M. P. (2017b). Catchment attributes for large-sample studies. Boulder, CO: UCAR/NCAR. <https://doi.org/10.5065/D6G73C3Q>
- Bárdossy, A., & Anwar, F. (2022). Why our rainfall-runoff models keep underestimating the peak flows? *Hydrology and Earth System Sciences Discussions*, 1-30.

- Bennett, A., & Nijssen, B. (2021). Deep learned process parameterizations provide better representations of turbulent heat fluxes in hydrologic models. *Water Resources Research*, 57(5), e2020WR029328.
- Beven, K. (2020). Deep learning, hydrological processes and the uniqueness of place. *Hydrological Processes*, 34(16), 3608-3613.
- Beven, K. J. (2000). Uniqueness of place and process representations in hydrological modelling. *Hydrology and Earth System Sciences*, 4(2), 203-213.
- Boulmaiz, T., Guermoui, M., & Boutaghane, H. (2020). Impact of training data size on the LSTM performances for rainfall–runoff modeling. *Modeling Earth Systems and Environment*, 6(4), 2153-2164.
- Chadalawada, J., Herath, H. M. V. V., & Babovic, V. (2020). Hydrologically informed machine learning for rainfall-runoff modeling: A genetic programming-based toolkit for automatic model induction. *Water Resources Research*, 56(4), e2019WR026933.
- Clark, M. P., Vogel, R. M., Lamontagne, J. R., Mizukami, N., Knoben, W. J., Tang, G., ... & Papalexiou, S. M. (2021). The abuse of popular performance metrics in hydrologic modeling. *Water Resources Research*, 57(9), e2020WR029001.
- Dutta, R., & Maity, R. (2020). Temporal networks-based approach for nonstationary hydroclimatic modeling and its demonstration with streamflow prediction. *Water Resources Research*, 56(8), e2020WR027086.
- Dutta, R., & Maity, R. (2021). Time-varying network-based approach for capturing hydrological extremes under climate change with application on drought. *Journal of Hydrology*, 603, 126958.
- Fang, K., Kifer, D., Lawson, K., Feng, D., & Shen, C. (2022). The Data Synergy Effects of Time-Series Deep Learning Models in Hydrology. *Water Resources Research*, 58(4), e2021WR029583.
- Gauch, M., Mai, J., & Lin, J. (2021). The proper care and feeding of CAMELS: How limited training data affects streamflow prediction. *Environmental Modelling & Software*, 135, 104926.
- Govindaraju, R. S. (2000). Artificial neural networks in hydrology. II: hydrologic applications. *Journal of Hydrologic Engineering*, 5(2), 124-137.
- Gupta, A., Carroll, R. W., & Mckenna, S. M. (2022). Changes in Streamflow Statistical Structure across United States due to Recent Climate Change. [Preprint]. DOI: <https://doi.org/10.31223/X5B08J>
- Hastie, T., Tibshirani, R., & Friedman, J. (2009). The elements of statistical learning: data mining, inference, and prediction. *Springer Series in Statistics*. Springer New York.

- Herath, H. M. V. V., Chadalawada, J., & Babovic, V. (2021). Hydrologically informed machine learning for rainfall–runoff modelling: towards distributed modelling. *Hydrology and Earth System Sciences*, 25(8), 4373-4401.
- Iorgulescu, I., & Beven, K. J. (2004). Nonparametric direct mapping of rainfall-runoff relationships: An alternative approach to data analysis and modeling? *Water Resources Research*, 40(8).
- Karpatne, A., Ebert-Uphoff, I., Ravela, S., Babaie, H. A., & Kumar, V. (2018). Machine learning for the geosciences: Challenges and opportunities. *IEEE Transactions on Knowledge and Data Engineering*, 31(8), 1544-1554.
- Kiang, J. E., Gazorian, C., McMillan, H., Coxon, G., Le Coz, J., Westerberg, I. K., ... & Mason, R. (2018). A comparison of methods for streamflow uncertainty estimation. *Water Resources Research*, 54(10), 7149-7176.
- Kratzert, F., Herrnegger, M., Klotz, D., Hochreiter, S., & Klambauer, G. (2019a). NeuralHydrology–interpreting LSTMs in hydrology. In *Explainable AI: Interpreting, Explaining and Visualizing Deep Learning* (pp. 347-362). Springer, Cham.
- Kratzert, F., Klotz, D., Brenner, C., Schulz, K., & Herrnegger, M. (2018a). Rainfall–runoff modelling using long short-term memory (LSTM) networks. *Hydrology and Earth System Sciences*, 22(11), 6005-6022.
- Kratzert, F., Klotz, D., Herrnegger, M., & Hochreiter, S. (2018b). A glimpse into the Unobserved: Runoff simulation for ungauged catchments with LSTMs. In *Workshop on Modeling and Decision-Making in the Spatiotemporal Domain, 32nd Conference on Neural Information Processing Systems (NeurIPS 2018)*. 2-8 Dec.
- Kratzert, F., Klotz, D., Herrnegger, M., Sampson, A. K., Hochreiter, S., & Nearing, G. S. (2019b). Toward improved predictions in ungauged basins: Exploiting the power of machine learning. *Water Resources Research*, 55(12), 11344-11354.
- Kratzert, F., Klotz, D., Shalev, G., Klambauer, G., Hochreiter, S., & Nearing, G. (2019c). Benchmarking a catchment-aware long short-term memory network (LSTM) for large-scale hydrological modeling. *Hydrol. Earth Syst. Sci. Discuss*, 2019, 1-32.
- Le Coz, J., Renard, B., Bonnifait, L., Branger, F., & Le Boursicaud, R. (2014). Combining hydraulic knowledge and uncertain gaugings in the estimation of hydrometric rating curves: A Bayesian approach. *Journal of Hydrology*, 509, 573-587.
- Lees, T., Buechel, M., Anderson, B., Slater, L., Reece, S., Coxon, G., & Dadson, S. J. (2021). Benchmarking data-driven rainfall–runoff models in Great Britain: a comparison of long short-term memory (LSTM)-based models with four lumped conceptual models. *Hydrology and Earth System Sciences*, 25(10), 5517-5534.

Milly, P. C., Betancourt, J., Falkenmark, M., Hirsch, R. M., Kundzewicz, Z. W., Lettenmaier, D. P., & Stouffer, R. J. (2008). Stationarity is dead: Whither water management? *Science*, 319(5863), 573-574.

Moulin, L., Gaume, E., & Obled, C. (2009). Uncertainties on mean areal precipitation: assessment and impact on streamflow simulations. *Hydrology and Earth System Sciences*, 13(2), 99-114.

Nearing, G. S., Kratzert, F., Sampson, A. K., Pelissier, C. S., Klotz, D., Frame, J. M., ... & Gupta, H. V. (2021). What role does hydrological science play in the age of machine learning? *Water Resources Research*, 57(3), e2020WR028091.

Nearing, G. S., Pelissier, C. S., Kratzert, F., Klotz, D., Gupta, H. V., Frame, J. M., & Sampson, A. K. (2019). Physically Informed Machine Learning for Hydrological Modeling Under Climate Nonstationarity. *UMBC Faculty Collection*.

Newman, A. J., Clark, M. P., Sampson, K., Wood, A., Hay, L. E., Bock, A., ... & Duan, Q. (2015). Development of a large-sample watershed-scale hydrometeorological data set for the contiguous USA: data set characteristics and assessment of regional variability in hydrologic model performance. *Hydrology and Earth System Sciences*, 19(1), 209-223.

Newman, A., Sampson, K., Clark M. P., Bock A., Viger R. J., & Blodgett D. (2014). A large-sample watershed-scale hydrometeorological dataset for the contiguous USA. Boulder, CO: UCAR/NCAR. <https://dx.doi.org/10.5065/D6MW2F4D>

Razavi, S. (2021). Deep learning, explained: Fundamentals, explainability, and bridgeability to process-based modelling. *Environmental Modelling & Software*, 144, 105159.

Renard, B., Kavetski, D., Leblois, E., Thyer, M., Kuczera, G., & Franks, S. W. (2011). Toward a reliable decomposition of predictive uncertainty in hydrological modeling: Characterizing rainfall errors using conditional simulation. *Water Resources Research*, 47(11).

Sadler, J. M., Appling, A. P., Read, J. S., Oliver, S. K., Jia, X., Zwart, J. A., & Kumar, V. (2022). Multi-Task Deep Learning of Daily Streamflow and Water Temperature. *Water Resources Research*, 58(4), e2021WR030138.

Singh, R., Wagener, T., Van Werkhoven, K., Mann, M. E., & Crane, R. (2011). A trading-space-for-time approach to probabilistic continuous streamflow predictions in a changing climate—accounting for changing watershed behavior. *Hydrology and Earth System Sciences*, 15(11), 3591-3603.

Sivapalan, M., Yaeger, M. A., Harman, C. J., Xu, X., & Troch, P. A. (2011). Functional model of water balance variability at the catchment scale: 1. Evidence of hydrologic similarity and space-time symmetry. *Water Resources Research*, 47(2).

- Srivastava, N., Hinton, G., Krizhevsky, A., Sutskever, I., & Salakhutdinov, R. (2014). Dropout: a simple way to prevent neural networks from overfitting. *The Journal of Machine Learning Research*, 15(1), 1929-1958.
- Stephens, C. M., Marshall, L. A., Johnson, F. M., Lin, L., Band, L. E., & Ajami, H. (2020). Is past variability a suitable proxy for future change? A virtual catchment experiment. *Water Resources Research*, 56(2), e2019WR026275.
- Wagener, T., Sivapalan, M., Troch, P., & Woods, R. (2007). Catchment classification and hydrologic similarity. *Geography compass*, 1(4), 901-931.
- Wi, S., & Steinschneider, S. (2022). Assessing the physical realism of deep learning hydrologic model projections under climate change. *Water Resources Research*, e2022WR032123.
- Zhang, B., & Govindaraju, R. S. (2000). Prediction of watershed runoff using Bayesian concepts and modular neural networks. *Water Resources Research*, 36(3), 753-762.
- Zhang, B., & Govindaraju, R. S. (2003). Geomorphology-based artificial neural networks (GANNs) for estimation of direct runoff over watersheds. *Journal of Hydrology*, 273(1-4), 18-34.